Chemical Science

ROYAL SOCIETY OF CHEMISTRY

REVIEW

View Article Online
View Journal

Cite this: DOI: 10.1039/d5sc08985a

Electronic structure manipulation in electrocatalysis: mechanisms and design principles

Hangkai Shi, Yuanduo Li, Shuyi Pang, Aixin Ma, Jianping Lai * and Lei Wang *

Electrocatalysis is a novel technology that can convert intermittent renewable electrical energy into high-value chemical fuels or products, achieving efficient energy storage and conversion. In the electrocatalytic process, the electron transfer and chemical reactions occurring at the interface are regarded as the core processes. Their efficiency is fundamentally regulated by the electronic behavior of the catalyst. Currently, many reactions have improved their efficiency by regulating electron transfer. However, the underlying mechanisms remain unclear. This review focuses on key electronic-level scientific issues in electrocatalysis, aiming to provide in-depth theoretical insights for the design of high-performance electrocatalysts. First, we systematically analyze the root causes of low electron transfer efficiency and review recent strategies for optimizing electron transport through material design and interface engineering. Second, we delve into the challenges of precisely regulating electronic structures. Moreover, we focus on the regulation mechanisms of the electronic states of the active centers and reaction pathways using emerging methods, such as elemental doping and spintronics. Furthermore, we elaborate on the complexity of the interfacial electron-transfer process by analyzing the influences of interface engineering, bulk redox chemistry, and pulsed electrocatalysis strategies on the kinetics of interfacial charge transfer. Finally, we highlight the latest progress in electrocatalytic theoretical research, including the application and challenges of advanced methods, such as the grand canonical ensemble density functional theory and machine learning, in simulating reaction environments. They can reveal electronic-level reaction mechanisms and accelerate catalyst design. This review clarifies these key electronic-level issues and outlines future directions for multidisciplinary integration and development directions in this field.

Received 18th November 2025
Accepted 19th March 2026

DOI: 10.1039/d5sc08985a

rsc.li/chemical-science

Introduction

The increasingly severe energy and environmental crises pose significant challenges to global sustainable development.[1–4] As a pivotal approach enabling the utilization of renewable electricity to drive molecular transformations and achieve efficient clean energy storage, electrocatalysis has emerged as a frontier focus in international scientific research and industrial innovation.[5–7] The core value of electrocatalysis lies in the direct conversion of intermittent electrical energy into stable chemical bonds through electron-transfer processes at the catalyst–electrolyte interface. This perfectly aligns with the principles of "green chemistry" and the global strategic vision of "carbon peaking and carbon neutrality," thereby propelling the chemical industry toward an intelligent development path characterized by low energy consumption and low emissions.[8–15]

In electrocatalysis, electronic regulation refers to the precise modification of the electronic structure of the catalyst active sites through material design and interface engineering in order to optimize the adsorption/desorption behavior with reaction intermediates.[16–18] Therefore, electron regulation can improve the reaction rate, selectivity, and energy efficiency. Its core goal is to regulate the electronic properties of active sites, enabling them to better meet the moderate adsorption requirements described by the Sabatier principle.[19,20] Electronic regulation not only focuses on static electronic properties but also involves the evolution of electronic behavior under dynamic conditions. Fundamentally, the improvement in electrocatalytic performance can ultimately be attributed to the precise control of electron transfer pathways and energy barriers.

Despite the enormous application potential exhibited by electrocatalysis technology, its transition from laboratory-scale research to industrial applications remains arduous.[21–23] The current bottlenecks, such as high overpotential, poor selectivity control, and low Faraday efficiency, stem not merely from macroscopic material structures but more profoundly from microscopic scientific issues at the electronic level.[24–26] These problems are intertwined, forming a complex network of

Key Laboratory of Eco-chemical Engineering, Ministry of Education, International Science and Technology Cooperation Base of Eco-chemical Engineering and Green Manufacturing, College of Chemistry and Molecular Engineering, Qingdao University of Science and Technology, Qingdao 266042, P. R. China. E-mail: jplai@qust.edu.cn; inorchemwl@126.com

challenges. First, there is an inherent limitation in terms of electron transfer efficiency.[27–29] Slow electron transfer kinetics and competitive side reactions during multi electron processes result in low energy utilization efficiency, with a significant portion of electrical energy dissipated as heat.[30–34] Second, there exists a regulatory dilemma regarding the electronic structure of active sites. An ideal catalyst requires a well-balanced correlation between its electronic properties and the adsorption energies of key reaction intermediates; however, achieving such precise electronic tailoring is extremely challenging.[35–40] Third, complex electron transport behaviors occur at the solid–liquid interface. The combined effects of the electrical double layer structure, local pH value, ion migration, and interfacial electric field profoundly influence the charge exchange efficiency between reactants, intermediates, and the electrode surface.[41–45] Finally, a gap persists between theoretical simulations and real reaction conditions. Traditional computational models often neglect the effects of electrode potential, solvation effects and dynamic surface reconstruction, leading to limited ability to predict and explain experimental phenomena.[46–49]

These electronic-level challenges are not isolated. Instead, they are closely coupled with the catalyst's geometric structure, phase composition, defect engineering and other factors, collectively determining the final electrocatalytic performance.[50,51] Therefore, gaining an in-depth understanding and addressing these fundamental scientific issues from an electronic perspective constitute an indispensable pathway for achieving disruptive breakthroughs in electrocatalysis technology. This review aims to provide a systematic and in-depth examination of these core electronic-level problems and summarize the latest research progress in the field of electrocatalysis (Fig. 1). First, we dissect the kinetic bottlenecks in electron transfer pathways and discuss strategies such as band engineering and interface modification to enhance the efficiency of electron supply and utilization. Subsequently, we delve into precise regulation strategies for electronic structures and how they optimize intermediate adsorption to steer reaction pathways. Next, we focus on electron transport in the interfacial micro-environment, analyzing the effects of interface engineering, electrolyte regulation and advanced electrolysis strategies on the kinetics of cross-interface charge transfer. Finally, we review the latest progress and future challenges of cutting-edge theoretical methods in constructing the material–structure–environment–performance–structure–activity relationship and accelerating the discovery of new catalysts. By sorting out and prospecting these key issues, this review intends to provide a solid electronic-level theoretical foundation and innovative design paradigm for constructing next generation electrocatalytic systems with high efficiency, stability, and selectivity.

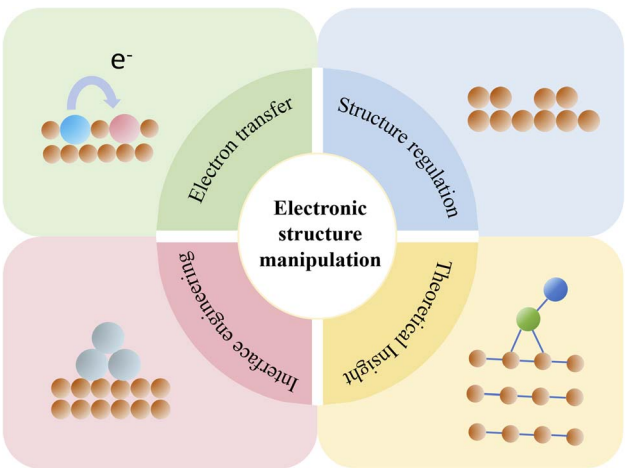

Fig. 1 Schematic of the electronic structure manipulation strategies in electrocatalysis.

Low electron transfer efficiency: issues and solutions

Manifestations and causes of poor electron transfer efficiency

Low electron transfer efficiency is the primary challenge in the field of electrocatalysis, directly impacting the reaction rate and energy conversion efficiency. In complex electrocatalytic reaction systems, intricate reaction mechanisms and the involvement of multiple electron transfer steps hinder electron transfer between the catalyst surface and reactants. This results in high reaction overpotential and substantial energy loss.[52–54] Charge transfer resistance (R_{ct}) serves as a crucial indicator for evaluating electron transfer efficiency. In electrocatalytic reactions, a smaller R_{ct} value signifies a faster electron transfer rate at the interface.[55–57]

Enhancing electron transfer efficiency

In recent years, researchers have proposed various strategies to enhance electron transfer efficiency, including constructing heterostructures, introducing defect sites, and optimizing catalyst conductivity.

Core–shell heterostructure design

Core–shell heterostructure design is one of the cutting-edge strategies for precisely regulating the electronic structure of catalysts and enhancing their electron transfer efficiency. This strategy constructs composite materials with well-defined interfaces by leveraging the differences in work function and electronic properties between the core and shell components to induce directional charge transfer at the interface. Consequently, the electronic states of the active sites are optimized, and reaction kinetics are significantly accelerated. For instance, Cheng *et al.* developed a bimetallic active site core–shell heterostructured catalyst (CSC-MoS_2@CoS_2), where edge-enriched MoS_2 nanosheet arrays were vertically grown on a cubic CoS_2 core (Fig. 2a). X-ray photoelectron spectroscopy (XPS) analysis revealed a shift of the Mo 3d peak toward higher binding energy, accompanied by a corresponding shift in the Co 2p peak (Fig. 2b and c), indicating efficient charge transfer from the CoS_2 core to the MoS_2 shell. This hierarchical design not only maximizes the exposure of active edge sites but also forms a tight heterointerface that synergistically modulates the electronic environment, thereby greatly facilitating electron transport during the electrocatalytic reaction.[58]

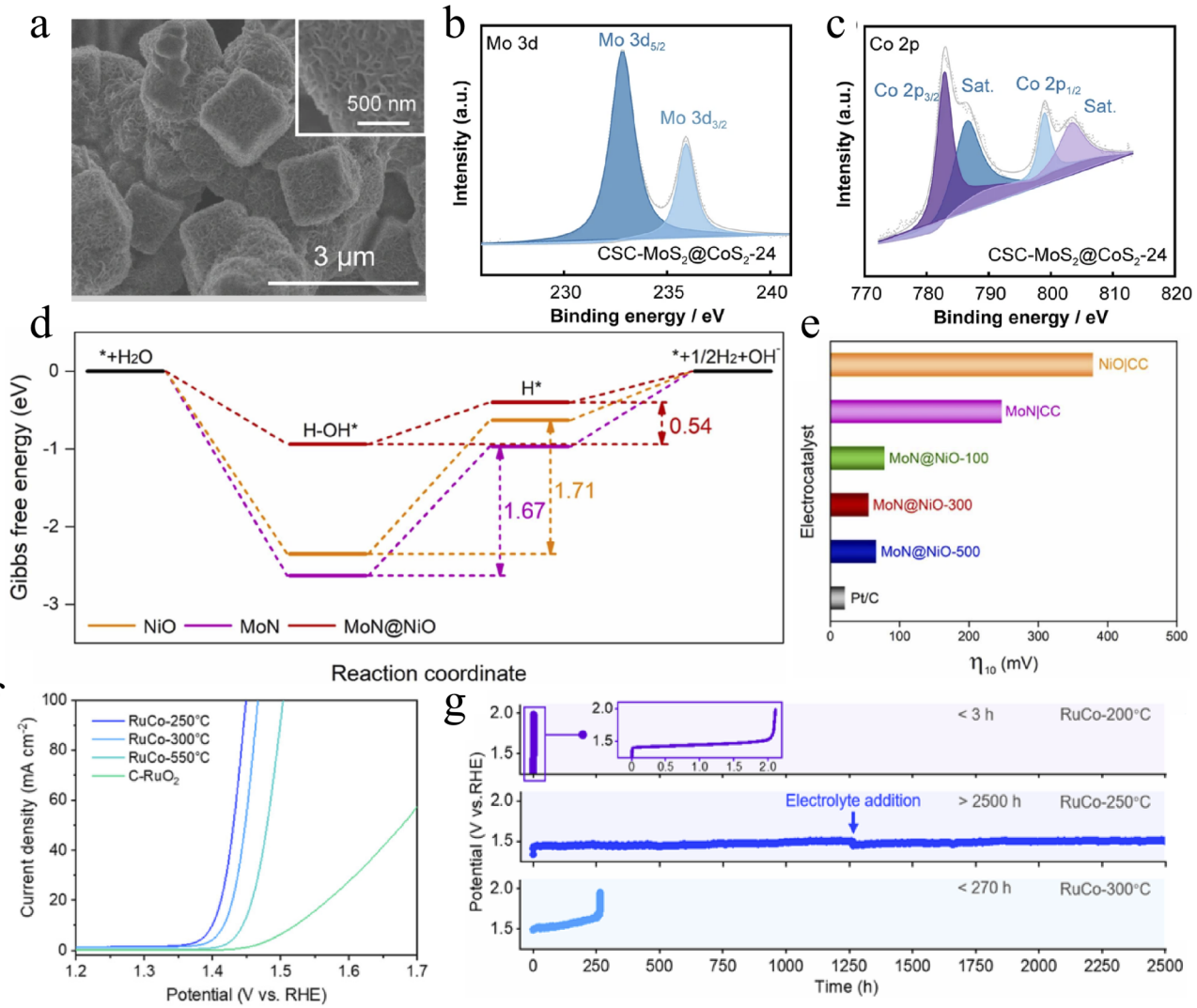

Fig. 2 (a) SEM images of CSC-MoS_2@CoS_2-24 at 3 μm (the magnification region is 500 nm of CSC-MoS_2@CoS_2-24). High-resolution XPS spectra of (b) Mo 3d and (c) Co 2p. (d) Gibbs free energy in each step. (e) η_{10}. (f) Polarization curves of RuCo-250 °C, RuCo-300 °C, RuCo-550 °C, and C–RuO_2. (g) Chronopotentiometric curves of the RuCo-alloy, RuCo-200 °C, and RuCo-250 °C at a current density of 10 mA cm^{-2} in a 0.5 M H_2SO_4 solution (the magnification region is the chronopotentiometric curves of RuCo-200 °C).

The MoN@NiO core–shell nanorod arrays developed by the Chen group constructed a directional charge transport pathway through the Mott–Schottky structure formed between the MoN core and NiO nanosheet shell. Density functional theory (DFT) calculations confirmed that this structure can effectively reduce the reaction barrier (Fig. 2d). MoN@NiO-300 achieved an overpotential of 55 mV at 10 mA cm^{-2} in the alkaline hydrogen evolution reaction (HER), with performance comparable to that of commercial Pt/C (Fig. 2e).[59] Furthermore, targeting the harsh environment of the acidic oxygen evolution reaction (OER), the Cao group designed a RuCo/$RuCoO_x$ core–shell Schottky heterojunction. Through the synergistic effect of the ultra-thin depletion layer and the core–shell interface, the electronic structure of the Ru active sites was regulated *via* lattice strain and charge transfer. This suppressed the oxidation of Ru and increased the electron transfer rate by an order of magnitude. An overpotential of 170 mV at 10 mA cm^{-2} and a long stability of 2500 hours were achieved in 0.5 M H_2SO_4 (Fig. 2f and g).[60]

Rare earth element doping

Rare earth element doping is a pivotal strategy for regulating the electronic structure of catalysts to enhance their electron transfer efficiency. Owing to the unique 4f electronic configuration, variable oxidation states and excellent oxygen storage of rare earth elements, their incorporation into the catalytic matrix can effectively modulate the charge distribution of active sites, optimize the adsorption strength of reaction intermediates, and significantly accelerate the kinetics of interfacial charge transport.

Feng *et al.* designed an atomically dispersed Gd-doped CuO_x catalyst (Gd_1/CuO_x). This catalyst uses the unique 4f electronic orbital and large ionic radius of Gd to introduce tensile strain into the CuO_x lattice and stabilize the critical Cu^+ active sites. *In*

situ X-ray absorption spectroscopy (XAS) measurements demonstrated that the single atom Gd doping maintained the Cu^{+} content at 85% under reductive conditions (Fig. 3a). DFT calculations further confirmed that the synergistic effect of tensile strain and Gd-induced electronic modulation reduced the formation energy barrier of *OCCO, which is the key intermediate for C–C coupling (Fig. 3b). This catalyst achieved a Faraday efficiency (FE) of 81.4% for C_2 products at −0.8 V *vs.* RHE and operated stably for over 40 hours at 500 mA cm^{-2}, providing an efficient pathway for the selective synthesis of multi-carbon products (Fig. 3c and d).[61]

Wang *et al.* broke the long range ordered structure of IrO_2 through Nd doping, constructing a Nd–IrO_2 catalyst with long range disorder but short range order. The incorporation of large radius Nd induces lattice strain, and the formed Nd–O–Ir bonds regulate the d-band center of Ir. Meanwhile, this structure weakens the excessively strong adsorption of active oxygen intermediates, increases the oxygen vacancy content, and activates the lattice oxygen mechanism to accelerate the reaction kinetics (Fig. 3e). In acidic media, the catalyst achieves an overpotential of only 263 mV at 10 mA cm^{-2}, and its stability at 50 mA cm^{-2} extends from 3 hours to 20 hours (Fig. 3f and g).[62]

CQD modification

Carbon quantum dot (CQD) modification has been widely proven as a universal strategy to significantly enhance the electron transfer efficiency of catalysts. Endowed with a unique nanoscale size, high specific surface area, and excellent intrinsic electrical conductivity, CQDs exhibit tremendous potential in the field of electrocatalytic energy conversion. When introduced into catalytic systems as functional components, CQDs act as efficient electron conductors to construct

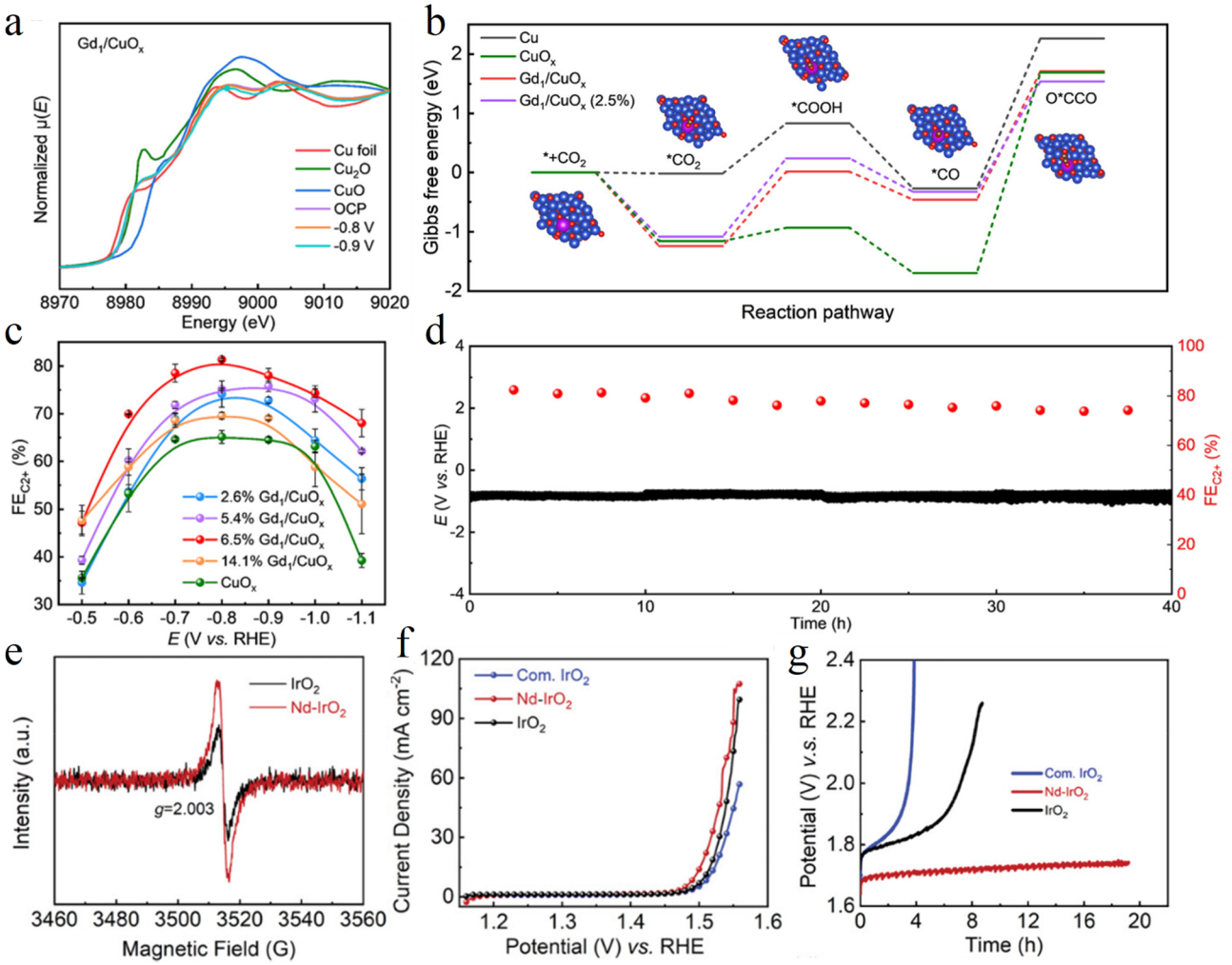

Fig. 3 (a) *In situ* XANES spectra at the Cu K-edge of Gd_1/CuO_x under different potentials; (b) Gibbs free energy diagrams of CO_2 reduction to O*CCO on the surfaces of Cu, CuO_x, Gd_1/CuO_x, and Gd_1/CuO_x (2.5%), insets are the schematic diagram of the adsorption configurations of various intermediates on the catalyst; (c) FEs for C_{2+} products over Gd_1/CuO_x with different Gd contents and CuO_x under different potentials; (d) long-term stability of 6.5% Gd_1/CuO_x at a constant current density of 500 mA cm^{-2}; (e) EPR spectra of Nd–IrO_2 and IrO_2; (f) LSV curves of Nd–IrO_2, IrO_2 and commercial IrO_2 in 0.5 M H_2SO_4 (scan rate: 5 mV s^{-1}); and (g) long-term electrochemical durability of $NdIrO_2$, IrO_2 and commercial IrO_2 (CP test at 50 mA cm^{-2}).

rapid electron transfer channels and interact strongly with the host material through their surface functional groups. This interaction optimizes the electronic structure of active sites while providing abundant defect sites to create more active centers.

The incorporation of CQDs into NiFe LDH for the OER serves as a paradigmatic example of electronic structure regulation. Surjith *et al.* designed a CQD/NFL/CNT catalyst, where interfacial electronic interactions between CQDs and NiFe LDH induce electron transfer from NiFe sites to CQDs. This charge rearrangement effectively optimizes the d-band electronic structure of Ni active sites, reduces the adsorption energy barrier for oxygen-containing intermediates, and thus inherently accelerates the electron transfer process of the rate determining step (RDS).[63]

CQDs can also serve as catalytic substrates. For instance, Lu group successfully constructed a highly active catalyst for the hydrogen evolution reaction (HER) by supporting Ru nanoparticles on CQDs. The incorporation of Ru not only modifies the charge distribution on the CQD surface but also, through its synergistic interaction with the carbon skeleton, significantly promotes the proton-coupled electron transfer (PCET) process. This endows Ru@CQDs with metal-like efficient electron transfer capability in acidic media.[64]

Experimental evaluation and theoretical simulation of electron transfer efficiency

To evaluate electron transfer efficiency, researchers have employed a variety of experimental methods and theoretical simulation approaches.

Electrochemical impedance spectroscopy

Electrochemical impedance spectroscopy (EIS) is an indispensable and powerful tool for elucidating reaction kinetics at electrode interfaces and evaluating electron transfer efficiency. By measuring the impedance response of the electrode system under alternating current signals of different frequencies, it can decouple complex electrochemical processes into a combination of distinct circuit components. This enables the quantitative analysis of the kinetic characteristics of processes such as charge transfer, interfacial transport and diffusion. Specifically, the diameter of the semicircle in the high frequency region of the Nyquist plot directly corresponds to the charge transfer resistance of the electrode reaction. A smaller resistance value typically indicates a lower energy barrier and higher efficiency for the electron transfer process.

For instance, in an alkaline HER, the synergy of electron proton transport at the double functional interface can be comprehensively analyzed through the combination of EIS and

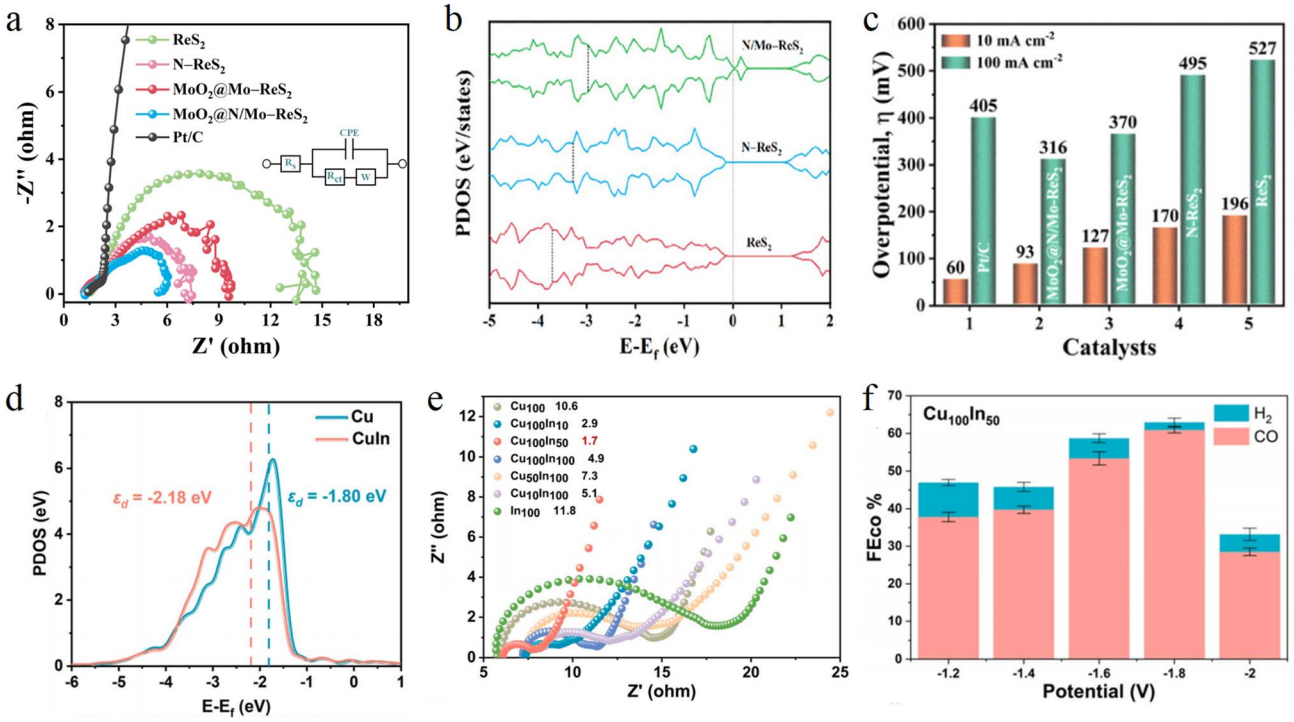

Fig. 4 (a) Nyquist plots of the corresponding electrocatalyst for the HER, inset is the circuit diagram; (b) PDOS analysis of ReS_2, N–ReS_2 and N/Mo–ReS_2 (PDOS: projected density of states. It represents the probability distribution of electrons on specific atomic orbitals, which can intuitively reflect the electronic occupancy state of the catalyst's active sites); (c) overpotential of ReS_2, N–ReS_2, MoO_2@Mo–ReS_2, MoO_2@N/Mo–ReS_2 and Pt/C; (d) d-band center of the active site of Cu and Cu_xIn_y (d-band center: the average energy position of the d orbitals in a metal catalyst is a key factor in regulating the adsorption strength of intermediates on the catalyst surface. The position of the d-band center relative to the Fermi level determines the strength of adsorption between the catalyst and the intermediates. Generally, the higher the d-band center, the stronger the adsorption); (e) Nyquist plots of the Cu_xIn_y–(COOH)CNTs catalysts; and (f) FE of the $Cu_{100}In_{50}$–(COOH)CNTs catalysts at different voltages.

DFT calculations. Singh *et al.* designed a MoO_2@N/Mo–ReS_2 catalyst. The EIS measurements revealed that its R_{ct} is 5.6 Ω, which is lower than that of pristine ReS_2 (Fig. 4a). This confirms that the strongly coupled interface between MoO_2 and ReS_2 not only accelerates water molecule dissociation but also optimizes the transport pathway of H intermediates. DFT calculations further verify that N and Mo co-doping upshifts the p-band of ReS_2, enhancing adsorption compatibility with H (Fig. 4b). Ultimately, it achieved a 93 mV low overpotential at 10 mA cm^{-2} (Fig. 4c).[65] In the electrochemical reduction of CO_2, Wang *et al.* synthesized a Cu–In–(COOH) CNT catalyst, where In doping downshifts the d-band center of Cu (Fig. 4d). This electronic structure modulation not only significantly reduces charge transfer resistance (Fig. 4e) but also increases the HER energy barrier and optimizes the CO_2 activation pathway. Ultimately, the catalyst achieves a CO FE of 60.9% at −1.8 V (Fig. 4f).[66]

Electron paramagnetic resonance

Electron paramagnetic resonance (EPR) is a powerful spectroscopic technique that directly detects and quantitatively analyzes unpaired electrons in materials. In electrocatalytic research, EPR probes the resonance signals of unpaired electrons to directly obtain the following key information: (1) the structure and concentration of paramagnetic active centers; (2) changes in electron spin states induced by interfacial charge transfer; and (3) the formation and evolution of key intermediates. Thus, EPR provides direct spectroscopic evidence for understanding the structural activity relationship between electron transfer efficiency and catalytic activity.

In the OER, the EPR measurements of the oxygen vacancy-rich V_O-$CoMoVO_x$ catalyst clearly observe a paramagnetic center signal attributed to electrons trapped by oxygen vacancies. Studies have demonstrated that the intensity of this signal significantly enhances and decays slowly after applying an external potential. This directly confirms that oxygen vacancies act as electron reservoirs during the reaction. They can trap and store electrons, effectively delaying electron dissipation and recombination. This behavior provides a stable electron supply for multi-step reactions, thereby improving the OER stability.[67]

DFT calculations

DFT calculations have emerged as an indispensable theoretical tool for uncovering electron transfer pathways and intrinsic mechanisms in catalytic processes at atomic and electronic scales. They can transcend the limitations of experimental characterization, intuitively predict charge rearrangement at interfaces and quantitatively evaluate the adsorption behavior of reaction intermediates. This provides profound theoretical insights and design guidelines for enhancing electron transfer efficiency.

For single atom catalysts in the oxygen reduction reaction (ORR), DFT calculations can accurately track how spin state evolution regulates electron transfer pathways. Yu *et al.* designed a Fe–N–C catalyst with constant potential DFT calculations demonstrating a dynamic spin state transition at the FeN_4 active sites. At low overpotentials ($U < 0.3$ V *vs.* SHE), the Fe centers predominantly adopt a medium spin state ($S = 1$), with an energy barrier of 0.35 eV for electron transfer from the d_{xz} orbital to the *OOH intermediate (Fig. 5a). When the potential increases to 0.3–1.5 V, the spin state switches to a high spin state ($S = 3/2$), enhancing the delocalization of d orbital electrons and reducing the electron transfer energy barrier to 0.21 eV (Fig. 5b). At this stage, FeN_4HS–OH becomes the dominant active site. This spin state-regulated electron transfer mechanism significantly improves the ORR half wave potential of the catalyst compared to systems without spin state optimization.[68]

In the electrocatalytic CO_2 reduction reaction, DFT calculations play a crucial role in analyzing the electronic synergy mechanism of dual active sites. In their study on CO_2-to-ethanol conversion using the CuNi@C/N-npG catalyst, Zhang *et al.* employed DFT calculations to reveal the strong metal–support interaction between the Ni–N–C support and the CuNi alloy. Electrons transfer from Cu to Ni and the N-npG support, leading the surface Cu to form $Cu^{\delta+}$ species (Fig. 5c and d). The d-band center of these $Cu^{\delta+}$ species upshifts by 0.15 eV compared to pure Cu, optimizing the electronic coupling strength between CH_3 and *CO intermediates (Fig. 5e). This electronic structure modulation promotes the electron transfer step in C–C coupling, allowing the FE of ethanol to remain ≥60% over a wide potential window (Fig. 5f).[69]

Challenges and breakthroughs in regulating electronic structures

Importance and difficulties of electronic structure regulation

The electronic structure of catalysts plays a decisive role in their catalytic performance. However, precisely regulating the electronic structure of catalysts constitutes a significant challenge. On one hand, the current understanding of the structure activity relationship between catalyst electronic structure and catalytic performance remains incomplete, making it difficult to accurately predict and design high efficiency catalysts with specific electronic structures through theoretical calculations and experimental methods. On the other hand, during actual electrocatalytic reactions, the electronic structure of catalysts is influenced by several factors, such as reaction conditions, reactant concentration and electrolyte properties. This makes it hard to ensure the stability of the electronic structure, thereby affecting the long-term performance of the catalysts.

Electronic structure regulation is crucial for optimizing the active sites and reaction pathways of catalysts. For instance, in electrocatalytic organic synthesis reactions, the electronic structure of catalysts directly influences the adsorption mode of reactive species on active sites, which in turn affects reaction activity and selectivity. Studies have shown that the activity and selectivity of electrocatalytic organic synthesis are related not only to the adsorption strength of reactant molecules but also to their adsorption configurations. In the reduction of Ph-NO_2 to Ph-NH_2 over Pd-based catalysts, multiple proton-coupled electron transfer steps are involved. DFT calculations demonstrate

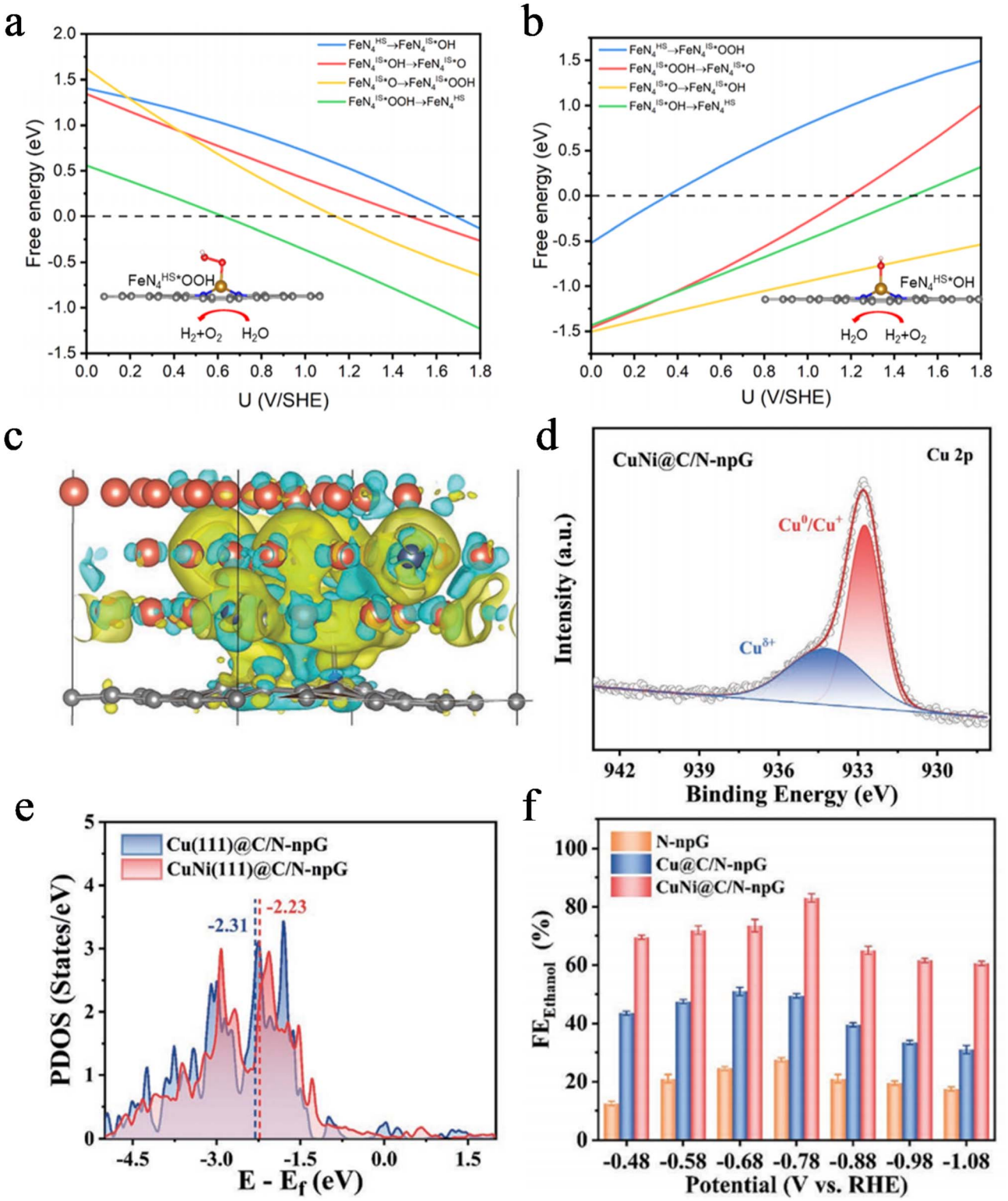

Fig. 5 (a) OER reaction calculated with different potentials in FeN_4HS*OOH, inset is the adsorption configuration of *OOH on FeN_4HS; (b) ORR reaction free energy with different potentials in FeN_4HS*OH, inset is the adsorption configuration of *OH on FeN_4HS; (c) charge density difference plots of CuNi(111)@C/N-npG; (d) high-resolution Cu 2p XPS spectra of CuNi@C/N-npG; (e) calculated partial density of states (PDOS) of the surface Cu atoms on CuNi(111)@C/N-npG (in red) and Cu(111)@C/N-npG (in blue); and (f) FE and the product distribution at different polarization potentials.

that Ph-NO_2 can adopt two adsorption configurations on the Pd surface: N atom-end vertical adsorption or benzene ring-plane parallel adsorption. The former facilitates the activation and cleavage of the N–O bond, while the latter may lead to incomplete hydrogenation or byproduct formation. Minor changes in the electronic structure of the catalyst can alter the ratio of these two adsorption configurations, thereby directly affecting the selectivity toward the aniline. This highlights the difficulty and necessity of regulating electronic structures to guide the formation of desired adsorption configurations.[70]

Electronic structure regulation

In recent years, researchers have proposed various methods for regulating electronic structure, including strategies such as alloying, heterojunction formation and oxygen vacancy engineering.

Alloying

Alloying is a powerful method for precisely regulating the electronic structure of catalysts by integrating two or more metal elements and leveraging the electronic interactions between their atoms. Its core mechanism lies in the inherent electronegativity difference between different metal elements, which drives directional electron transfer at the interface, directly altering the electron density and d-band structure of active sites. This fine-tuning of the electronic structure optimizes the adsorption strength of reactants and intermediates on active sites, making it more consistent with the Sabatier principle. Consequently, it not only enhances reaction activity but also significantly improves the reaction pathway and selectivity.

For instance, in the BiCu single atom alloy (BiCu-SAA) designed by Zhang's group, the reverse electron transfer from single atom Bi to Cu upshifts the d-band center of Cu (Fig. 6a). This enhancement strengthens the adsorption and coupling capability of *CO intermediates, leading the Faraday efficiency of C_{2+} products to reach 73.4% (Fig. 6b).[71] In the Ag–Cu biphasic catalyst developed by Gao *et al.*, *CO intermediates induce dynamic interfacial reconstruction, driving electrons to transfer from Ag to Cu-enriched regions and enabling the dynamic regulation of Cu's d-band center during the reaction. The Cu-enriched interface exhibits a higher d-band center, which promotes ethylene formation. As the Ag proportion increases, the d-band center downshifts, favoring alcohol production instead. This achieves precise regulation of C_{2+} products (Fig. 6c and d).[72]

Li *et al.* prepared a face-centered cubic (fcc) Fe–Pd alloy *via* electrochemical dealloying. They leveraged electron transfer between Pd and Fe to shift the d-band center of Pd away from the Fermi level by 0.2 eV, weakening the Pd–H bond strength. This optimization adjusts the Gibbs free energy of the H* intermediate from −0.36 eV to −0.15 eV (Fig. 6e). In a 1 M KOH electrolyte, the catalyst achieves an overpotential of only 58 mV at 10 mA cm^{-2}, outperforming commercial Pt/C (Fig. 6f).[73] Lai group synthesized a CuPt alloy *via* simple electrodeposition, where the electronegativity difference between Cu and Pt induces electron transfer from Cu to Pt. This electronic reconstruction optimizes the d-band structures of both Cu and Pt, enhancing the adsorption and dehydration capabilities of Pt sites toward HCOOH. In contrast, Cu sites better facilitate the formation and adsorption of *NH_2 intermediates, with the two sites exerting a synergistic effect. At a current density of −502.3 mA cm^{-2}, the catalyst achieves a urea FE as high as 58.1%, demonstrating the pivotal role of alloying in boosting the electrocatalytic C–N coupling performance for urea synthesis.[74]

In summary, this alloying-enabled electronic synergy demonstrates tremendous potential across noble and non-noble metal systems. Future efforts should combine machine learning with *in situ* characterization to track dynamic electronic evolution under working conditions.

Heterojunction

Constructing heterojunctions is a cutting edge strategy for regulating the electronic structure of catalysts, with its core lying in the atomic scale integration of two or more semiconductor or conductor materials with distinct band structures. When these materials come into contact, directional charge transfer occurs at the interface to achieve Fermi level equilibrium, thereby forming a built-in electric field generated by carrier diffusion and a corresponding space charge region. This microstructural feature exerts two key effects on catalytic processes. First, the built-in electric field acts like a built-in electron pump, providing a strong driving force for the separation and cross interface transfer of electrogenerated carriers, significantly enhancing electron utilization efficiency. Second, the space charge region induces opposite charge distributions on both sides of the heterojunction. This functional zoning enables differential adsorption and activation of different reactants, paving the way for precise regulation of reaction pathways in complex reaction systems.

For instance, Yang *et al.* synthesized heterostructured MoO_2–FeP *via in situ* growth combined with low temperature phosphidation, using it as a bifunctional catalyst for the HER and 5-hydroxymethylfurfural (HMF) oxidation. Electrons transfer from MoO_2 to FeP, leading to electron enrichment in the FeP phase, which endows it with an optimal H* adsorption energy (Fig. 7a). The electron deficient MoO_2 phase better facilitates HMF oxidation. The electrolyzer driven by this bifunctional catalyst requires only a low voltage of 1.486 V to simultaneously produce H_2 and FDCA at 10 mA cm^{-2}, outperforming the noble metal Pt/C benchmark (Fig. 7b) and enabling direct power supply by solar cells.[75]

In the CoP/CeO_2 heterojunction designed by Jiang *et al.*, electrons transfer from CoP to CeO_2, forming a built-in electric field at the interface that points from CeO_2 to CoP (Fig. 7c and d). During the OER, this built-in electric field powerfully drives electrons to rapidly transfer from the active sites on the CoP side to CeO_2 and ultimately flow to the electrode. This significantly accelerates the formation rate of high valent active species (CoOOH) on Co sites and suppresses charge recombination, enabling the heterojunction to exhibit an OER activity far exceeding that of its individual components (Fig. 7e).[76] For MoS_2 catalysts, their HER activity mainly originates from edge

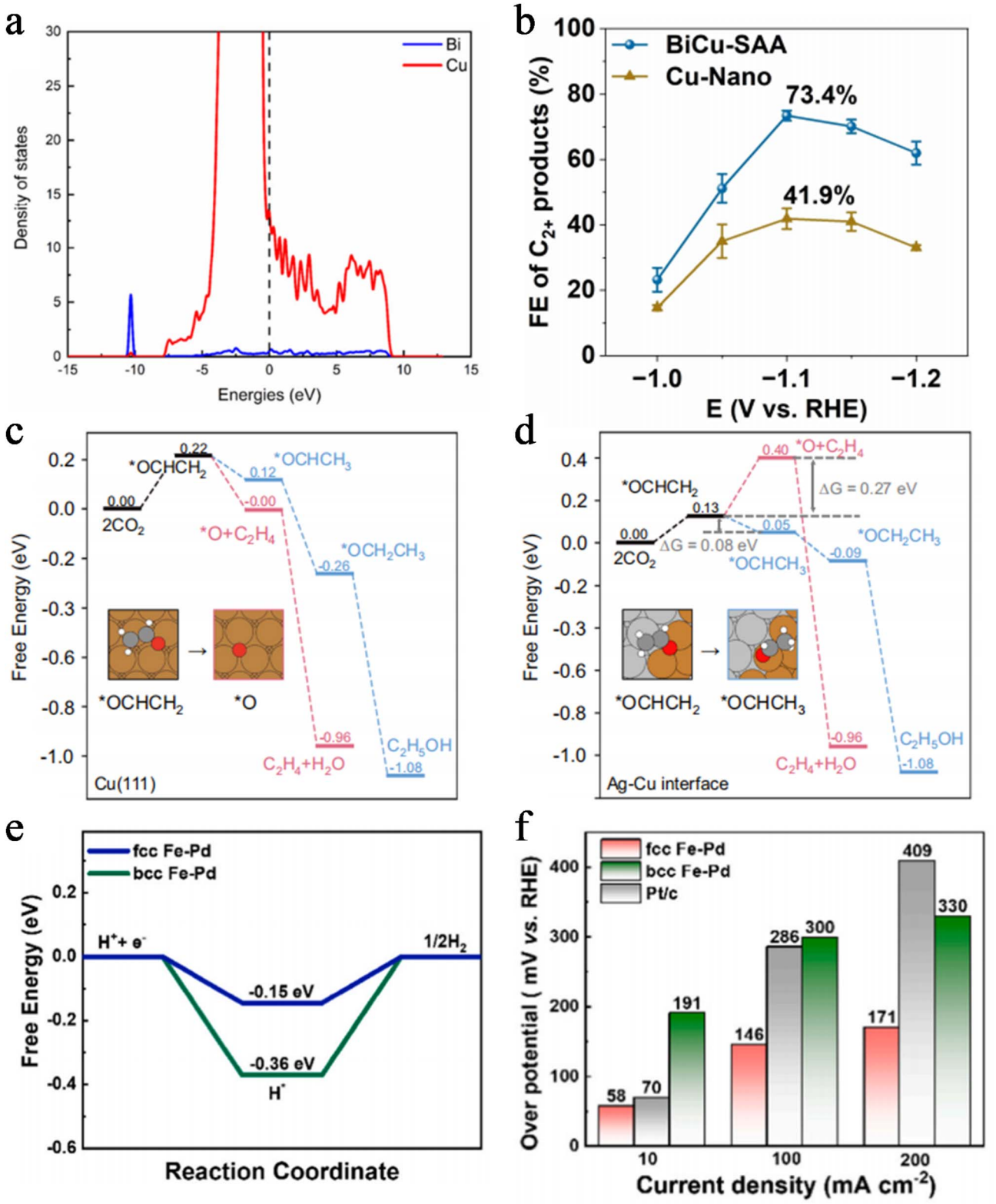

Fig. 6 (a) PDOS results for the BiCu(111)-SAA slab; (b) FE values of C_{2+} products on the BiCu-SAA and control Cu-nano catalysts at different applied potentials in an H-type cell. Reaction profile for the C_2H_4 path and C_2H_5OH path on (c) Cu(111) and the (d) Ag–Cu interface, inset is the adsorption configuration of different intermediates on Cu(111) and Ag–Cu interface; (e) hydrogen-free energies of systems; and (f) overpotential of fcc Fe–Pd at different current densities.

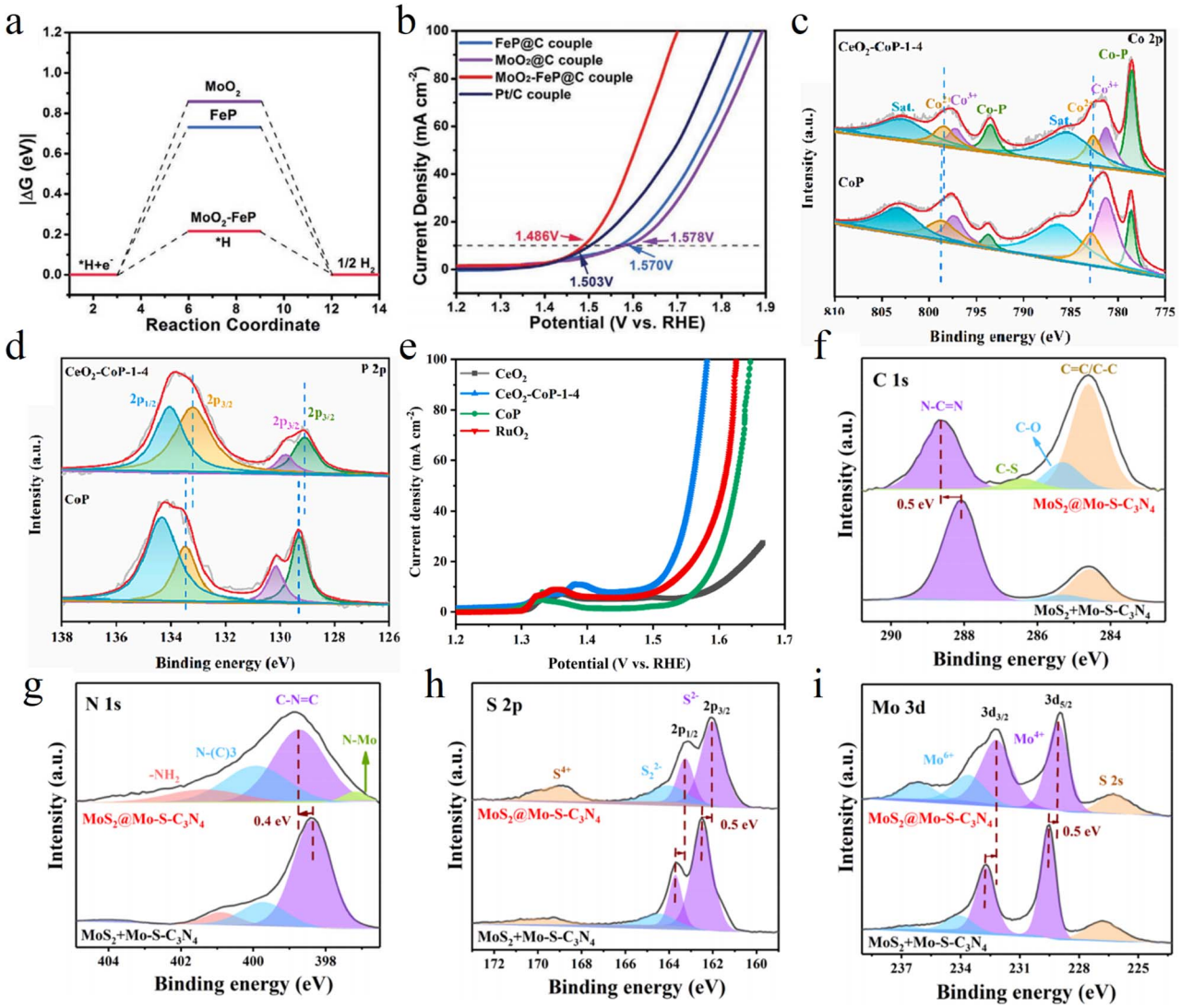

Fig. 7 (a) H* adsorption energy of MoO_2–FeP, FeP, and MoO_2 systems; (b) polarization curves of the FeP@C, MoO_2@C, MoO_2–FeP@C, and Pt/C couples in 1.0 M KOH with 10 mM HMF. XPS survey spectra of (c) Co 2p and (d) P 2p. (e) Polarization curves (with 95% *iR* correction) of CeO_2–CoP-1-4, CeO_2 CoP and RuO_2. XPS of (f) C 1s, (g) N 1s, (h) S 2p and (i) Mo 3d regions with fitting curves for MoS_2 + Mo–S–C_3N_4 and MoS_2@Mo–S–C_3N_4.

sites, while the extensive basal plane remains inert. After constructing the MoS_2/g-C_3N_4 van der Waals heterojunction, interfacial electronic interactions induce electron redistribution from g-C_3N_4 to the basal plane region of MoS_2 (Fig. 7f–i). This successfully activates the S atoms on the MoS_2 basal plane, turning them into the new HER active sites.[77]

By creating microdomains with complementary functions, heterojunction engineering provides an ideal platform for tandem and bifunctional catalysis. Future work should pursue an atomically precise interface design tailored to industrial current densities.

Oxygen vacancy

Introducing oxygen vacancies is a direct and efficient strategy for regulating the electronic structure of catalysts by creating anionic defects. The formation of oxygen vacancies generates a large number of coordination-unsaturated active sites and introduces local defect energy levels into the band structure of the material. This significantly alters the charge distribution, electronic conductivity and adsorption behavior of the catalyst toward reaction molecules. Such remodeling of the electronic structure enhances the catalyst's adsorption affinity for specific reaction intermediates and optimizes the reaction pathway, thereby achieving higher activity and target product selectivity in complex electrocatalytic reactions.

For instance, Zhou *et al.* reported a carbon-supported Ni/MoO_2 heterojunction catalyst. The introduction of oxygen vacancies in the MoO_2 lattice increases the electron density of Ni active sites through the strong electronic coupling effect between Ni and MoO_2, significantly enhancing the adsorption capacity for the phenol hydrogenation intermediate $C_6H_5O^-$. It also reduces the competitive adsorption between H* and the

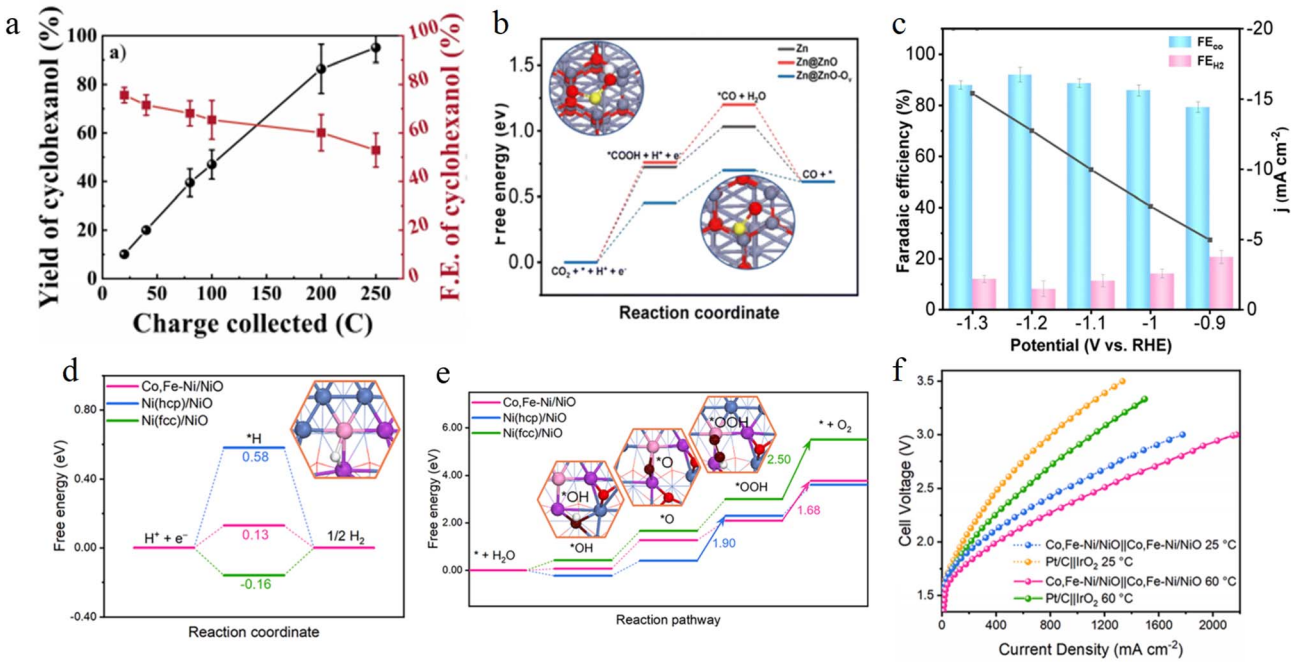

Fig. 8 (a) Summary of long-term electrolysis results obtained at 60 °C in a solution containing 0.10 M H_2SO_4 and 20 mM phenol with Ni_{10}@MoO_2; (b) free-energy diagrams of CO_2RR to CO on Zn, Zn@ZnO and Zn@ZnO–O_v, inset is the adsorption configuration of different intermediate on catalysts; (c) product FEs and current densities for Zn@ZnO-650 at different potentials; and (d) free energy diagrams for the HER on the catalyst surfaces. The inset shows the adsorption configuration of *H on Co and Fe–Ni/NiO. (e) Free energy diagrams for the OER on the catalyst surfaces. The insets show the adsorption configurations of *OH, *O and *OOH species on Co and Fe–Ni/NiO. XPS of (f) polarization curves of the Co, Fe–Ni/NiO||Co, Fe–Ni/NiO and Pt/C||IrO_2 electrolyzers recorded at 25 and 60 °C in a 1.0 M KOH solution.

intermediate, enabling the FE of cyclohexanol to exceed 76% (Fig. 8a).[78] Xu's group designed a Zn@ZnO-*T* catalyst, where they regulated the oxygen vacancy content of ZnO by adjusting the sintering temperature. This regulation modulates the electron density of Zn sites, significantly enhancing the adsorption and activation capabilities of CO_2 and lowering the formation energy barriers of *COOH and *CO intermediates (Fig. 8b). Among these, the ZnO catalyst prepared at 650 °C achieves a CO FE of 92.1% in 0.1 M $KHCO_3$ (Fig. 8c), breaking the bottleneck of hydrogen evolution competition for traditional Zn-based catalysts under high current densities.[79]

Oxygen vacancies often synergize with heterointerfaces to construct hierarchical electron transport channels, simultaneously optimizing the HER and OER performance. Du *et al.* constructed an oxygen vacancy-rich Co-/Fe-doped metastable Ni/NiO heterojunction using a thermal shock method, in which oxygen vacancies and the Ni/NiO interface exert a synergistic electronic effect. The high energy electron configuration of metastable hcp-Ni accelerates charge transfer, while the vacancies optimize the adsorption energies of H* and O containing intermediates (Fig. 8d and e). The electrolyzer based on this catalyst achieves 10 mA cm^{-2} at 1.48 V and reaches an industrial level current density of 1.0 A cm^{-2} at 2.55 V (Fig. 8f).[80]

In summary, oxygen vacancies act as electron donors and create unique coordination environments. Future research should move from simply introducing vacancies to precisely controlling their concentration, spatial distribution, and dynamic evolution under reaction conditions.

Interfacial electron transfer issues and optimization strategies

Essence and impacts of interfacial electron transfer issues

The core of electrocatalytic reactions lies in the electron transfer process at the catalyst–electrolyte interface, and its efficiency and stability directly determine the performance ceiling of the entire reaction. However, interfacial electron transfer faces multiple challenges stemming from dynamic instability. First, in harsh electrochemical environments, catalytically active components tend to undergo dissolution and migration and trigger the agglomeration of nanoparticles *via* the Ostwald ripening process.[81–84] This not only reduces the active specific surface area but also destroys the continuous three-dimensional conductive network, increasing the electron transfer resistance between particles. Second, strongly adsorbed intermediates generated during the reaction irreversibly occupy active sites, forming an insulating or high-energy-barrier overlayer. This overlayer blocks the channels for reactant access and electron transfer both physically and electronically, causing severe catalyst poisoning.[85,86] Additionally, conductive carriers face corrosion risks. For instance, carbon materials oxidize under anodic potential, causing structural collapse and catalyst detachment. Even partial corrosion alters their surface chemical properties, which significantly increases the contact resistance between the carrier and the catalyst, and systematically raises the overall energy barrier for electron transport.[87–89] These

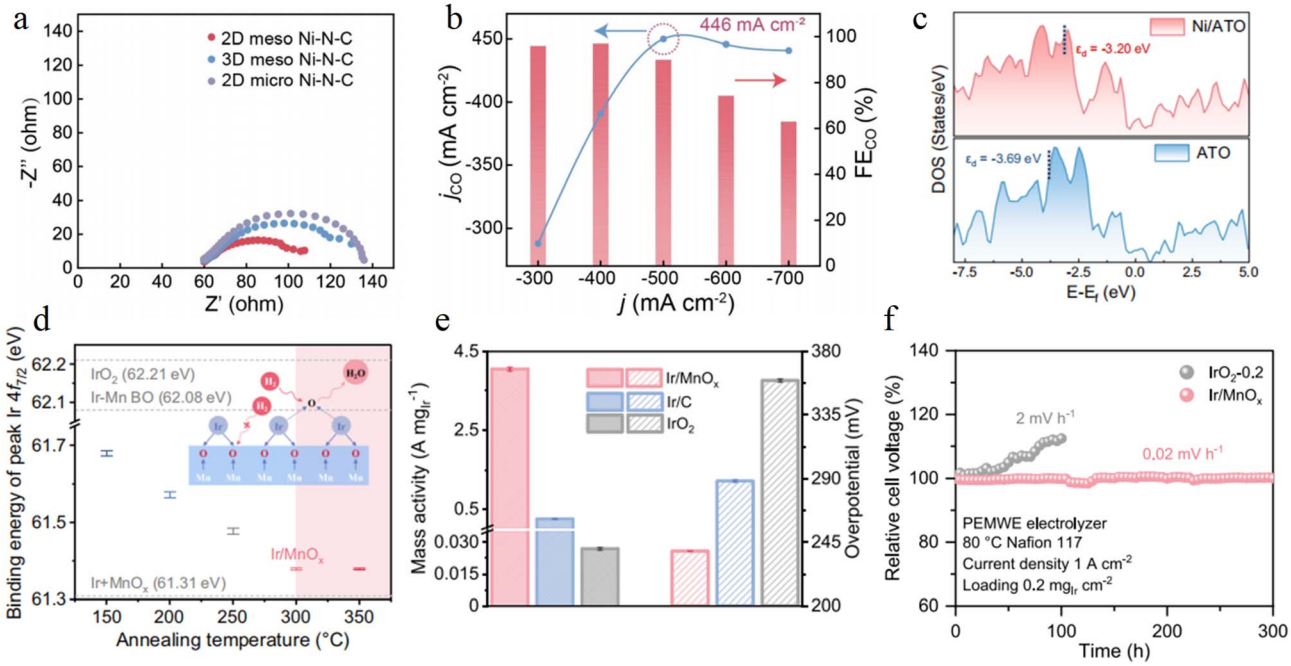

Fig. 9 (a) EIS spectra of 2D mesoporous Ni–N–C, 3D mesoporous Ni–N–C and 2D microporous Ni–N–C; (b) partial current density of CO (j_{CO}) curves and the FE_{CO} histogram of 2D mesoporous Ni–N–C under high current density in a gas-fed flow cell; (c) total DOS of ATO and Ni/ATO; and (d) binding energy of XPS Ir $4f_{7/2}$ peak as a function of the annealing temperature of the precursor with a 95% confidence interval. The inset indicates robust Ir–O–Mn bonds generated near the heterointerfaces after annealing; (e) mass activity at the overpotential of 300 mV and the overpotential at 10 mA cm^{-2} of Ir/MnO_x, Ir/C and IrO_2; and (f) chronopotentiometry curves at a current density of 1.0 A cm^{-2} of Ir/MnOx and IrO_2-0.2.

degradation mechanisms collectively lead to a sustained increase in interfacial impedance and rapid decay of reaction kinetics, forming a critical interfacial electron transport bottleneck that must be addressed for the practical application of electrocatalytic technologies.

Interface engineering

To address interfacial electron transport issues, researchers have proposed diverse interface engineering strategies, including single atom and nanocluster deposition, interface modification, and interfacial structure regulation.

Single atom and nanocluster deposition

Single atom and nanocluster deposition is a revolutionary strategy for precisely regulating and maximizing interfacial electron transport efficiency. Such catalysts anchor metals on supports in the form of isolated atoms or ultrasmall clusters composed of several atoms, achieving nearly 100% atomic utilization efficiency. They exhibit exceptional electrocatalytic performance due to their unique quantum confinement effect and maximum active interface area. Researchers have successfully fabricated supported single atom and cluster catalysts with well-defined structures through various strategies, including spatial confinement, wet chemical impregnation, and electrochemical deposition. Among these, carbon-based materials with excellent electrical conductivity and chemical stability are widely used as ideal supports. The bonding modes between metal active centers and supports mainly fall into two categories: direct anchoring and indirect loading *via* bridging atoms, like oxygen. This precise bonding establishes strong electronic interactions and atomic scale interfaces between metals and supports. It not only greatly stabilizes metal sites to prevent their migration and agglomeration but also constructs a highly efficient electron transport channel, thereby significantly enhancing interfacial electron transfer efficiency and optimizing the adsorption behavior of reaction intermediates.

In CO_2 electroreduction, Ni single atoms supported on N-doped carbon (Ni–N–C) achieve directional regulation and efficient transport of electrons *via* a planar Ni–N_4 coordination structure. Ma *et al.* developed a two-dimensional mesoporous Ni–N–C catalyst through an interface assembly strategy. Ni single atoms directly anchor to the carbon framework *via* four Ni–N bonds, and the high electronegativity of N atoms drives electron transfer from Ni to the N-doped carbon support. The EIS results show that this catalyst exhibits much lower charge transfer resistance than its three-dimensional mesoporous counterpart, with the electron transfer rate between Ni active sites and the carbon support increasing by more than 3 times (Fig. 9a). In flow cells, its CO partial current density reaches 446 mA cm^{-2} (FE_{CO} > 95%), which confirms that the directly anchored Ni–N bonds provide a low resistance channel for electron transport (Fig. 9b).[90] In another study, Zhang group immobilized Ni single atoms on ATO supports *via* magnetron sputtering, forming Ni–O–Sb electron transfer bridges through bridging bonds. The 3d orbitals of Ni single atoms couple with

the Sb 5s orbitals of ATO *via* O atoms, directing electron transfer from the ATO support to Ni sites through the O bridge, which upshifts the d-band center of Ni (Fig. 9c) and enhances the adsorption and dissociation capacity of water molecules. The fast electron channel established by this bridging structure significantly improves both hydroxyl radical generation efficiency and charge transfer rate compared to pure ATO, enabling the efficient mineralization of refractory organics in high salinity wastewater treatment.[91]

Guo group designed porous IrO_x/MnO_x nanosheets that achieve indirect loading *via* Ir–O–Mn bridging bonds, where IrO_x nanoclusters and MnO_x supports form a dense bridged interface. The Ir–O–Mn bonds act as efficient charge transfer channels, facilitating the directional transport of electrons (Fig. 9d). The EIS measurements show that this catalyst has a much lower charge transfer resistance than commercial IrO_2. In 0.5 M H_2SO_4, it exhibits an overpotential of 238 mV at 10 mA cm^{-2} and a mass activity of 4 A mg_{Ir}^{-1} (Fig. 9e). Furthermore, it operates stably for 300 hours at 1 A cm^{-2} in a PEM electrolyzer, with an Ir leaching rate of only 1.81% (Fig. 9f).[92]

Interface modification

Interface modification is a critical strategy for precisely regulating the electronic structure of catalysts and optimizing interfacial electron transport. It not only enhances the stability of active components by constructing specific chemical bonds or functional groups between supports and active sites, but it also reshapes the interfacial charge distribution through the electronic coupling effect, thereby significantly boosting electron transfer efficiency and catalytic reaction kinetics.

Liu *et al.* designed an interfacial Pt–O–C structure, anchoring Pt single atoms on highly curved onion-like carbon (OLC) supports to construct the Pt_1/OLC catalyst. DFT calculations show that the unique curvature of OLC induces a strong local electric field at the Pt sites, significantly reducing the energy barrier for water dissociation and facilitating hydrogen adsorption/desorption processes (Fig. 10a). Meanwhile, the Pt–O–C bonds formed between Pt atoms and the support not only provide stable anchoring sites but also act as highly efficient electron transport channels, allowing the catalyst to exhibit exceptional activity in acidic media (Fig. 10b).[93]

Jiao group constructed the $Cr_{0.02}Ni(OH)_{2+\delta}$ catalyst *via* Lewis acid Cr doping. The introduction of Cr forms a Cr–O–Ni-

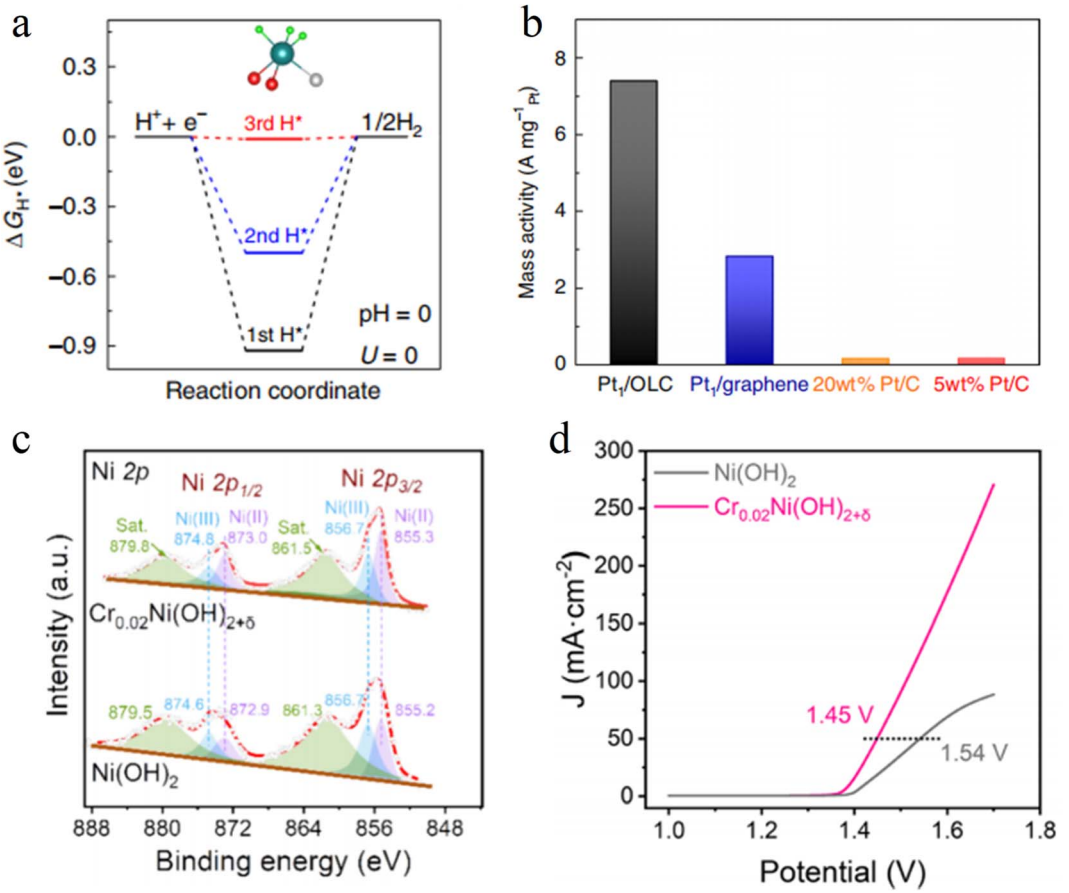

Fig. 10 (a) Calculated free-energy diagram of the HER at the equilibrium potential with pH = 0 and assuming that Pt is the active site. The inset shows the model of H adsorbed on the Pt site, where light green, green, red and grey balls represent hydrogen, platinum, oxygen and carbon atoms, respectively. (b) Mass activity of Pt_1/OLC is normalized to the Pt loading at an η of 38 mV with respect to the reference catalysts; (c) high-resolution XPS spectra of Ni 2p for $Ni(OH)_2$ and $Cr_{0.02}Ni(OH)_{2+\delta}$; and (d) LSV curves of the $Ni(OH)_2$, and $Cr_{0.02}Ni(OH)_{2+\delta}$ for the MOR.

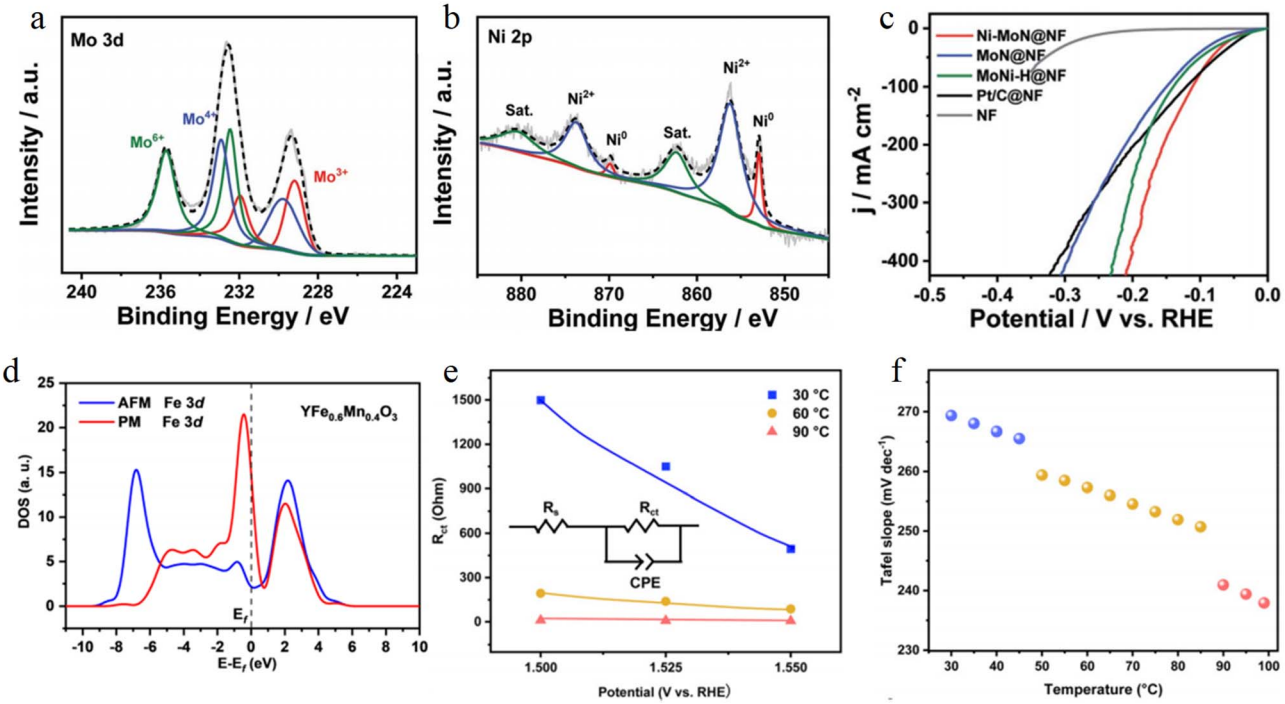

Fig. 11 (a) High-resolution Mo 3d XPS spectra of the Ni–MoN@NF; (b) high-resolution Ni 2p XPS spectra of the Ni–MoN@NF; (c) HER polarization curves of all catalysts in 1 M KOH; (d) projected DOS of Fe 3d orbitals at antiferromagnetic and paramagnetic $YFe_{0.6}Mn_{0.4}O_3$; and (e) temperature-dependent R_{ct} fitted from the EIS data in the potential regions of water oxidation. The inset shows the Randle's equivalent circuit. (f) Temperature-dependent Tafel slopes.

modified interface on the surface of $Ni(OH)_2$, markedly altering the electronic microenvironment of the active centers. The strong electropositivity of Cr^{3+} induces electron transfer from Ni to Cr *via* O bridges, rendering Ni sites electron-rich (Fig. 10c) and enhancing the adsorption capacity for OH^-. DFT calculations show that Cr modification reduces the energy barrier for methanol dissociation. At 1.55 V *vs.* RHE, its current density is three times higher than that of pure $Ni(OH)_2$, with the onset potential shifting negatively by 120 mV (Fig. 10d).[94]

Zou group converts antiferromagnetic $YFe_{0.6}Mn_{0.4}O_3$ to a paramagnetic state *via* thermal excitation, forming a magnetically disordered $YFe_{0.6}Mn_{0.4}O_3$@YFeOOH interface. XPS results show that the binding energy of interfacial Fe^{3+} increases, and the electronic density of states is enhanced at the Fermi level (Fig. 11d). Thermal excitation reduces the spin flip barrier by 60%, lowers the charge transfer resistance from 180 Ω to 25 Ω, and decreases the OER Tafel slope from 120 mV dec^{-1} to 65 mV dec^{-1} (Fig. 11e and f).[96]

Interfacial structure regulation

Interfacial structure regulation is a critical strategy for enhancing electrocatalytic performance, as it enables the effective optimization of electron transport pathways and reaction energy barriers through the precise design of the interfacial structure at the atomic scale. In recent years, researchers have constructed abundant atomic interfacial active sites in various transition metal-based heterogeneous catalysts *via* atomic interface engineering, thereby significantly boosting electrocatalytic performance.

Sun *et al.* developed the Ni–MoN@NF catalyst *via in situ* phase separation technology, where the interface between metallic Ni and MoN forms synergistic sites. XPS results show that the binding energy of Ni 2p decreases whereas that of Mo 3d increases, indicating that the built-in electric field accelerates charge transport (Fig. 11a and b). In 1 M KOH, the catalyst exhibits an overpotential of only 37.36 mV at 10 mA cm^{-2} (Fig. 11c).[95]

Effects of bulk water redox chemistry on interfacial electron transport

In recent years, researchers have discovered that bulk water redox chemistry plays a critical role in interfacial electrocatalytic processes, breaking the limitations of traditional electrocatalytic theories that strictly confine reactions to the electrode–electrolyte interface.

Traditional electrocatalytic theories regard bulk aqueous electrolytes merely as a source of reaction environment, protons and oxygen. Although this classic model greatly simplifies the electrocatalytic system, it also overlooks the potential active role that the bulk solution can play. In recent years, groundbreaking experimental evidence has revolutionized this paradigm.

Cui *et al.* successfully built a bridge between bulk solution redox chemistry and interfacial electrocatalysis. Multidimensional experimental evidence confirms that water itself is no longer an inert solvent but an active redox reaction medium that

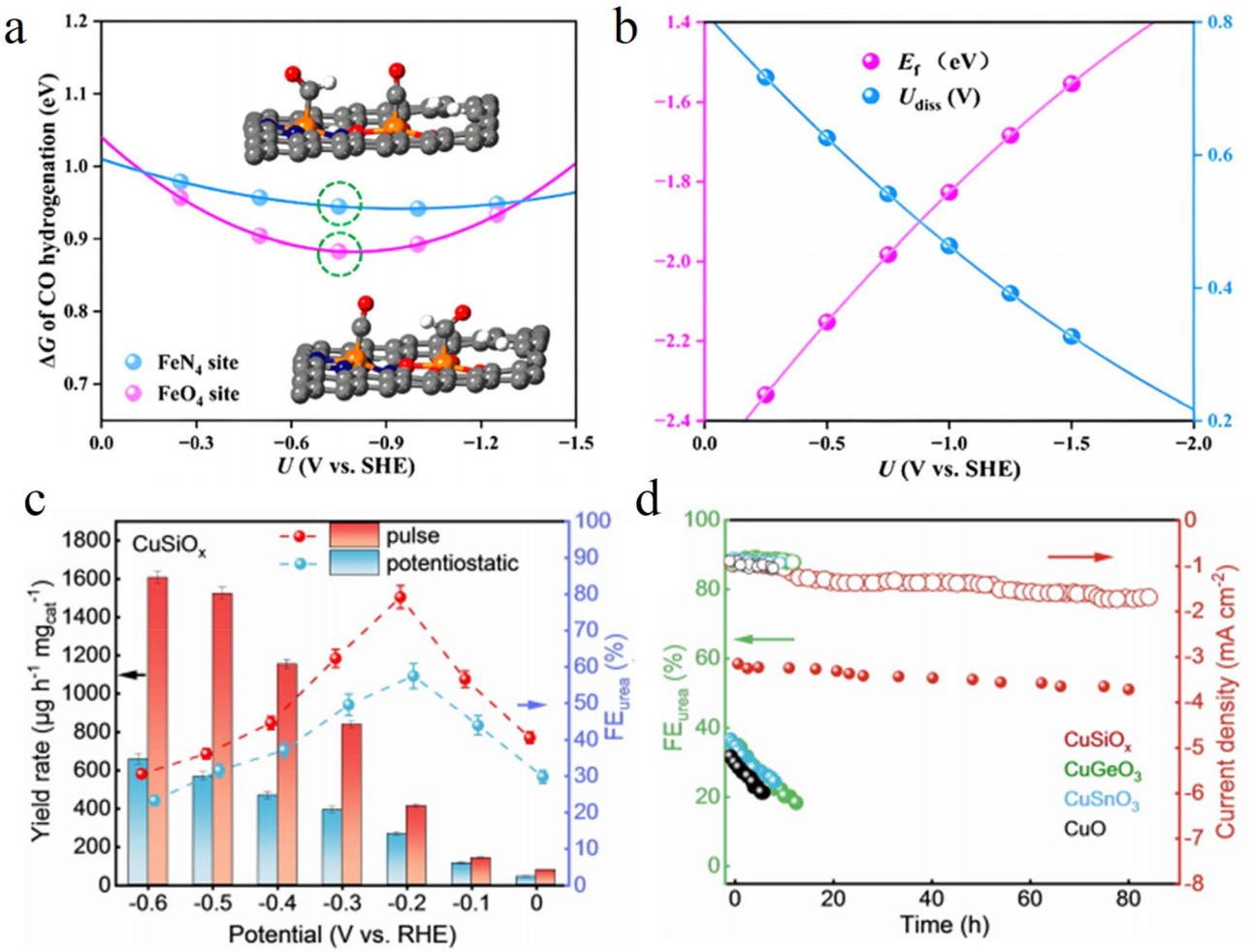

Fig. 12 (a) ΔG values of CO hydrogenation on FeN_4 and FeO_4 sites as functions of applied potentials (ΔG: the change in Gibbs free energy. It is used to assess the thermodynamic feasibility of elementary reactions in electrocatalysis. The closer the ΔG value is to 0, the more readily the reaction can occur spontaneously), inset is the adsorption configuration of different intermediate on FeN_4 and FeO_4 sites. (b) E_f and U_{diss} values of the SAN at different applied potentials; (c) FEs and yields of urea corresponding to $CuSiO_x$ at different potentiostatic and pulse potentials; and (d) stability performance diagrams of the four catalysts.

can participate in and regulate interfacial electron transport. Taking a formate electrolyte and Cu catalysts as the model, the research team has verified *via* various advanced characterization techniques that formate ions in the electrolyte can disrupt the hydrogen bond network of bulk water, inducing water to generate various redox radicals. These water-derived radicals can directly oxidize formate in the bulk solution and continuously produce key C_1 reaction intermediates, such as $^{\bullet}CO_2$ and $^{\bullet}CO$. Furthermore, these freely generated C_1 intermediates in the solution can migrate to the surface of the copper electrode, utilize Cu sites for C–C coupling, and ultimately yield multicarbon products.[97]

Pulsed electrocatalytic strategy

As a cutting edge approach for regulating interfacial electron transport, the pulsed electrocatalytic strategy breaks through the limitations of traditional potentiostatic and galvanostatic modes. By precisely manipulating changes in the electrode potential over the time dimension, it achieves dynamic optimization of the interfacial electric double layer structure, coverage of reaction intermediates, and electron transport pathways. The core of this strategy lies in utilizing potential pulses with specific frequency and amplitude to periodically alter the interfacial electric field environment, thereby breaking the constraints of traditional steady state catalysis.

In pulsed sequential electrocatalysis design, researchers elaborately design pulse sequences to decouple complex multistep reactions into independent steps performed at different potentials. For electrocatalytic CO_2 reduction, Sun *et al.* alternately applied reductive and oxidative potentials. This achieves efficient CO_2 conversion during the reductive phase and removes poisoned species accumulated on the catalyst surface during the oxidative phase (Fig. 12a). Meanwhile, they regulate the interfacial proton concentration, significantly enhancing the selectivity and stability of C_{2+} products (Fig. 12b).[98] This temporal regulation not only addresses issues such as insufficient reactant supply and difficult product desorption in

traditional steady state operations but also regulates the interfacial electronic density of states to optimize the electron transfer energy barriers of key steps.

In electrochemical urea synthesis, the pulsed strategy also offers a novel regulatory dimension. The Zhang group developed a $CuSiO_x$ nanotube catalyst with an atomic scale Cu–O–Si interface, actively regulating the dynamic equilibrium of Cu^+/Cu^0 *via* periodic pulsed potentials. During the reductive phase, Cu^0 sites efficiently adsorb CO_2 to generate *CO intermediates. In the oxidative phase, the in situ-formed Cu^+ species optimize the adsorption configuration of NO_2^-, achieving dynamic regulation of the C–N coupling energy barrier. In a flow electrolyzer, it achieves a urea yield of 1606.1 μg h^{-1} $mg_{cat.}^{-1}$ and an FE of 79.01% (Fig. 12c). Moreover, the FE for urea retains over 80% during an 80 hour stability test (Fig. 12d), significantly outperforming most reported catalysts.[99]

Progress and challenges in theoretical research on electrocatalysis

Limitations of theoretical research on electrocatalysis

In recent years, experimental research in the electrocatalysis field has made remarkable progress, yet no unified electrocatalytic theory has emerged to guide the design and development of new electrocatalysts. For some complex electrocatalytic phenomena and electronic-level issues, such as the dynamic evolution of electronic states and interfacial electric field effects, in-depth theoretical analysis and quantitative description are lacking. This leaves experimental research without theoretical guidance, making it difficult to achieve breakthrough progress.

One of the major challenges in the field of electrocatalysis is the disconnection between theory and experiment. DFT calculations are widely used in electrocatalysis research, but traditional DFT calculations usually proceed under the condition of a constant number of electrons, making it difficult to accurately describe the charge transfer process in electrocatalytic reactions. In addition, electrocatalytic reactions involve complex

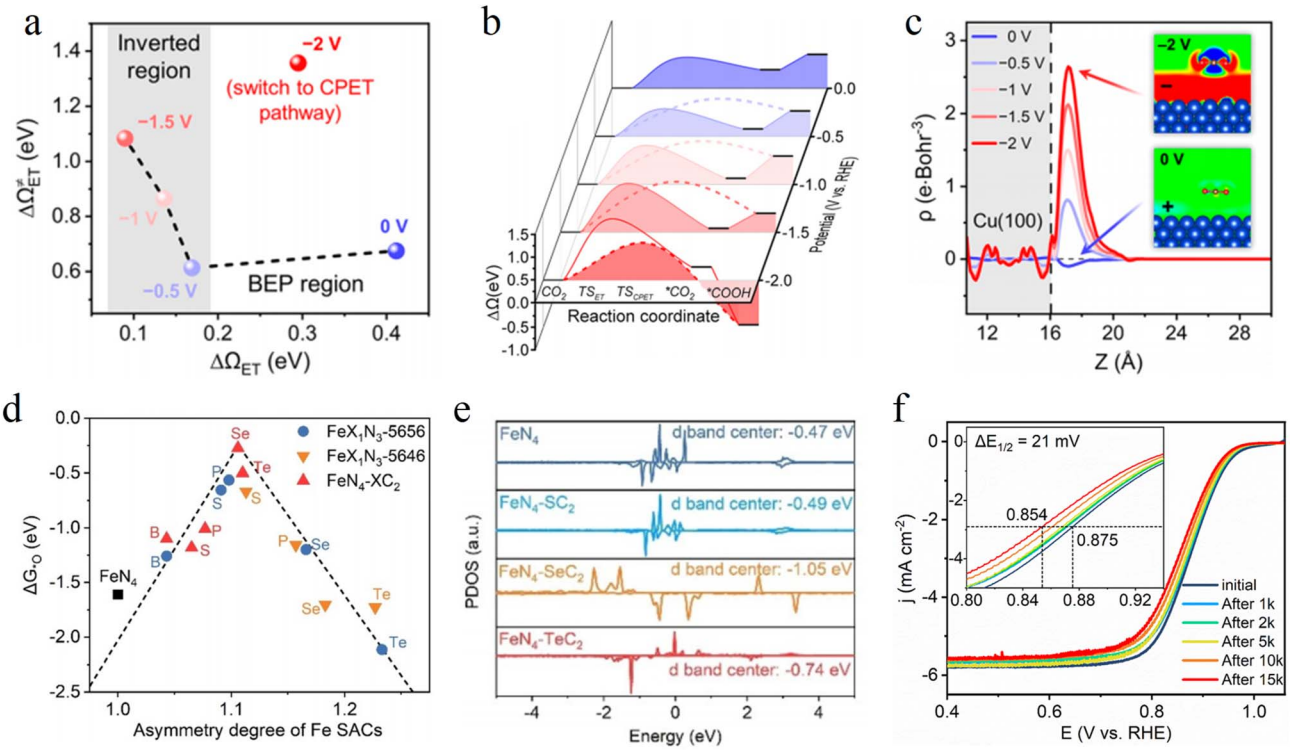

Fig. 13 (a) Correlation between the grand free-energy barrier of the ET step ($\Delta\Omega_{ET}^{\ddagger}$) and the ET reaction free energy ($\Delta\Omega_{ET}$) on Cu(100), which shows a BEP region from 0 V to −0.5 V but a sharply inverted region from −0.5 V to −1.5 V (ET step: electron transfer step. The process in which electrons are directionally transferred between the catalyst active sites, reaction intermediates, and the electrolyte/electrode. ET reaction free energy: a core parameter for quantitatively describing the thermodynamic trend of a certain ET step; it refers to the change in Gibbs free energy of the system when a single-step electron-transfer reaction is completed under constant temperature and pressure); (b) grand free energy profiles of CO_2 activation in the eCO_2RR on Cu(100) at U = 0 V, −0.5 V, −1 V, −1.5 V, −2 V (RHE scale at pH = 7) through the SEPT and CPET mechanisms illustrated at the bottom; (c) interfacial net charge densities on the Cu(100) surface relative to the PZC condition from 0 V to −2 V (the dashed line marks the surface), inset is the state density plot; (d) correlation between ΔG_{*O} and asymmetry degree; (e) projected density of state (PDOS) of the Fe single-atom; and (f) long-term durability tests of FeN_4–SeC_2. The inset shows a magnified section.

multi-step processes, and theoretical calculations cannot fully consider all factors.

Applications of GCE-DFT

To address the limitations of traditional DFT calculations, GCE-DFT has emerged. GCE-DFT extends computational simulations from the canonical ensemble to the grand canonical ensemble, with its core idea treating the electron number of the system as a variable and imposing a constant electronic chemical potential. Using this approach, GCE-DFT can directly simulate the charge distribution, reaction energy barriers, and stability of reaction intermediates at the catalyst–electrolyte interface under a constant applied potential. It thus directly incorporates the potential into quantum mechanical calculations, enabling more realistic and accurate simulations of electrocatalytic processes.

Xiao group combines GCE-DFT with an implicit electrolyte model to systematically investigate the electron transfer mechanism of CO_2 activation on Cu surfaces and identifies a potential-dependent Marcus inversion region. The calculations show that under regular operating potentials, CO_2 activation follows the SEPT mechanism. The Fermi level of Cu exhibits high matching with the lowest unoccupied molecular orbital (LUMO) of CO_2, and the electron transfer energy barrier is below 0.5 eV (Fig. 13a). In contrast, when the potential drops below −1.2 V, the Fermi level shifts significantly downward, inducing strong Pauli repulsion between the occupied states of Cu and the highest occupied molecular orbital (HOMO) of CO_2. This causes a sharp increase in the energy barrier of the SEPT pathway (Fig. 13b). The reaction switches to the CPET mechanism out of necessity. The GCE-DFT-derived charge density difference plots intuitively reveal this potential-dependent orbital interaction. Under negative potentials, the efficiency of electron density transfer from the Cu surface to CO_2 decreases (Fig. 13c). Along with the reduced adsorption energy of the *CO intermediate, this ultimately leads to increased H_2 selectivity.[100]

To address the trade-off between activity and stability of Fe–N–C ORR catalysts, Cao *et al.* combine GCE-DFT with machine learning to construct electronic structure models of asymmetric FeN_4 sites. The calculations show that the electron density of symmetric FeN_4 sites exhibits a centrosymmetric distribution, resulting in overly strong *OH adsorption (Fig. 13d). In contrast, asymmetric coordination lowers the d-band center of Fe by 0.58 eV (Fig. 13e) and reduces the peak density of states near the Fermi level. This optimizes the *OH adsorption energy and enhances the fracture resistance of the Fe–N bonds. The onset potential predicted by GCE-DFT matches the experimental value, and the catalyst retains over 95% of its activity after 15 000 cycles (Fig. 13f), confirming the decisive role of electron density regulation in catalytic performance.[101]

Asymmetric electrocatalysts

Zhang proposed a new paradigm for the design of asymmetric electrocatalysts, which stands as a milestone theoretical breakthrough in the field of electrocatalytic materials in recent years. The theory innovatively and systematically integrates the concept of asymmetric regulation into the electrocatalysis field by precisely constructing materials with compositional asymmetry, size asymmetry, coordination asymmetry, and multiple asymmetric structures at the atomic scale. This successfully breaks the inherent dilemma in traditional electrocatalytic materials.[102]

At the micro mechanism level, asymmetric regulation exhibits multi-dimensional synergistic effects. Compositional asymmetry achieves directional charge rearrangement through electronic interactions between different elements, optimizing the electronic structure of active sites. Size asymmetry constructs hierarchical structures at the nano to sub-nano scale, which not only accelerates the mass transfer of reactants and products but also stabilizes active centers *via* the spatial confinement effect. Coordination asymmetry breaks the traditional symmetric coordination environment to create active sites with unique electronic states, precisely regulating the adsorption behavior of reaction intermediates. When these asymmetric factors act synergistically through multiple asymmetric strategies, they generate significant synergistic enhancement effects across different scales, enhancing catalytic performance.

Zhang *et al.* developed asymmetric Pt–Ru–Co triatomic catalysts (Pt–Ru–Co TAs) *via* selective atomic layer deposition (ALD) technology, achieving ultrahigh noble metal utilization efficiency in a hydrogen oxidation reaction (HOR). DFT calculations show that the moderately electronegative Co atoms act as electronic bridges, transferring charge to Pt sites through Pt–Co and Ru–Co coordination bonds. The 5d-band center of Pt shifts up from −3.032 eV to −1.611 eV, enhancing the adsorption capacity for *H intermediates (Fig. 14a). *In situ* X-ray absorption near edge structure (XANES) confirms that Co exists in an oxidized state (Fig. 14b). Its 3d orbital unoccupied states form strong hybridization with the 5d occupied states of Pt, markedly boosting electron transfer efficiency. The catalyst exhibits an HOR mass activity of 2.89 A mg^{-1} at an overpotential of 50 mV, which is 57.8 times that of commercial Pt/C (Fig. 14c). Moreover, the current only decreases by 5% after 10 h of the HOR testing (Fig. 14d). This stability stems from the electronic coupling between heterogeneous metals suppressing the oxidative dissolution of Pt.[103]

Asymmetric electrocatalysts exhibit promising application prospects in key energy conversion systems, such as metal–air batteries and water splitting. Studies have shown that asymmetrically designed Co–N–C catalysts demonstrate excellent oxygen reduction and evolution bifunctional activity in Zn–air batteries, and their performance degradation rate is reduced by one order of magnitude compared with that of traditional symmetric catalysts.[104] These breakthroughs not only deepen the understanding of electronic-level mechanisms in electrocatalytic processes but also provide novel theoretical frameworks and design principles for developing next-generation high efficiency, stable electrocatalytic materials.

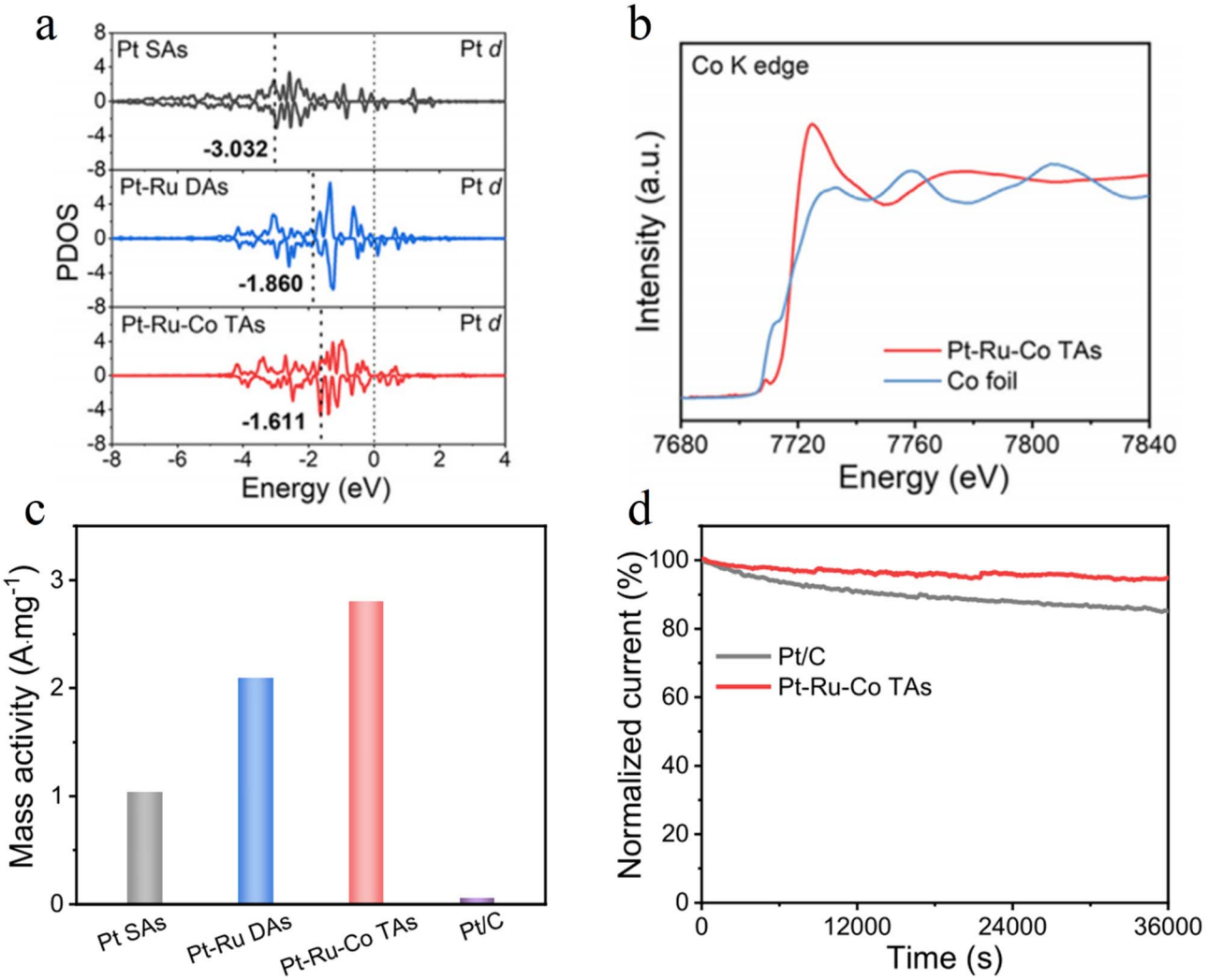

Fig. 14 (a) PDOS of Pt d bands in the three structural models. The positions of the dashed line represent the d-band center; (b) XANES of the Co K edge; (c) mass activities of Pt SAs, Pt–Ru DAs, Pt–Ru–Co TAs and Pt/C at an overpotential of 50 mV for the HOR; and (d) relative chronoamperometry response of Pt–Ru–Co TAs and Pt/C at 0.1 V (*vs.* RHE) in a H_2-saturated 0.1 M $HClO_4$ solution.

Machine learning in theoretical research

In recent years, machine learning has emerged as a transformative force, profoundly reshaping the theoretical research and design paradigms of electrocatalysts. Its greatest strength lies in its ability to efficiently mine the hidden laws of structure activity relationships from massive, high-dimensional experimental and theoretical data, thereby establishing accurate prediction models that link atomic structures and electronic properties with macroscopic catalytic performance.

Wang group developed the SurFF model, replacing traditional DFT calculations with deep learning force fields and boosting the efficiency of surface energy prediction by 10^5 times. While maintaining an accuracy of 3.0 meV $Å^{-2}$, the model performs a high-throughput correlative analysis of the electronic structures and surface exposure characteristics of thousands of alloy catalysts. This efficiency leap covers ground-state electronic properties and prioritizes the screening of high-information samples through active learning strategies. It builds high precision models with minimal computational resources, laying the foundation for the rapid development of non-noble metal catalysts.[105] Lian *et al.* combined machine learning potentials with large scale molecular dynamics simulations to reveal the dynamic oxygen migration mechanism of oxide-derived Cu catalysts in CO_2RR. They found that diffusion kinetics limit surface oxygen reduction, providing a new paradigm for modeling dynamic electronic behaviors.[106]

In summary, these advanced theoretical methods are transforming catalyst design from an empirical art into a predictive science. GCE-DFT bridges the gap between idealized computations and operating conditions by enabling simulations under constant potential, allowing researchers to screen catalysts based on their performance at realistic applied voltages. Machine learning, when combined with high throughput DFT, accelerates the discovery of structure property relationships, identifying the key electronic descriptors that govern activity and selectivity. The emerging paradigm of asymmetric

Table 1 Summary of electronic structure regulation strategies in electrocatalysis

Strategy	Examples	Design principle	Effects on electronic structure
Heterostructure engineering	Core–shell: MoS_2@CoS_2, MoN@NiO, RuCo/$RuCoO_x$ Heterojunction: MoO_2–FeP, CoP/CeO_2, MoS_2/g-C_3N_4	Interface electric field and charge separation	d-band center shift; charge redistribution; optimized adsorption energy of intermediates
Elemental doping	Rare-earth doping: Gd–CuO_x, Nd–IrO_2 Non-metal doping: N in ReS_2	Lattice distortion and band engineering	Tensile strain; stabilization of specific oxidation states; upshift/downshift of d-band center
CQD modification	CQDs/NiFe LDH/CNT; Ru@CQDs	Construction of low resistance conductive channels at the interface and expansion of active sites	Optimized d-band electronic structure; reduced adsorption energy barrier
Defect engineering	Oxygen vacancies: Ni/MoO_2, Zn@ZnO, Co/Fe–Ni/NiO	Local electronic state modulation	Localized electron density; altered Fermi level; optimized adsorption energy
Alloying	Single-atom alloy: BiCu Biphasic alloy: Ag–Cu Intermetallic: Fe–Pd, CuPt	Electronic synergy and strain effect	d-band center shift; optimized Gibbs free energy of intermediates
Single-atom and nanocluster deposition	Ni–N–C; IrO_x/MnO_x; Pt_1/OLC; Ni/ATO	Max atom utilization and strong metal–support interaction	Efficient charge-transfer channels; tuned oxidation states; upshifted d-band center
Interface modification	Cr–O–Ni; Pt–O–C	Interface microenvironment regulation, low-resistance electronic channel design	Electron-rich active sites; modified adsorption energy of reactants
Dynamic regulation	Pulsed electrocatalysis: $CuSiO_x$ Bulk water redox chemistry	Dynamic adaptation of reactions, regulation of external field timing, and dynamic restructuring induced by intermediates	Transient charge redistribution; regulation of interfacial proton concentration; adaptive electronic states

electrocatalysis provides a systematic framework to break linear scaling relations through deliberate symmetry breaking at the atomic scale, offering a pathway to circumvent the longstanding trade-offs between adsorption strength and reaction kinetics. Together, these approaches converge toward a design-by-descriptor paradigm, where catalysts are rationally engineered based on targeted electronic parameters rather than discovered through trial and error.

Conclusion and outlook

To facilitate a holistic understanding of the diverse electronic regulation strategies discussed in this review, Table 1 summarizes the key approaches, their design principles, and their effects on electronic structure.

Besides, this review has comprehensively examined four key electronic-level issues in the field of electrocatalysis. Through an analysis of the latest research advances, we draw the following conclusions and identify critical directions for future inquiry:

Low electron transfer efficiency is the primary challenge in the field of electrocatalysis, directly affecting reaction rates and energy conversion efficiency. Strategies such as constructing heterostructures, introducing defect sites, and optimizing catalyst conductivity can effectively enhance electron transfer efficiency. However, the fundamental limits of electron transport under practical high current density operations remain poorly understood. Future research efforts should focus on decoupling the contributions of conductivity and interfacial charge and on exploring materials with unconventional electronic band structures that may enable near lossless charge transport. The key contradiction to resolve is how to maintain ultrafast electron transfer while preserving catalyst stability and active site accessibility.

Difficulties in electronic structure regulation represent a key factor restricting the performance improvement of electrocatalysts. Approaches including alloying, doping, and heterojunction formation can efficiently modulate the electronic structure of catalysts, boosting their catalytic activity and selectivity. In particular, rare earth element doping, as an emerging strategy, exhibits unique advantages in regulating the electronic structure of catalysts. Nevertheless, the current understanding remains largely empirical; we still lack predictive control over electronic descriptors such as d-band center, spin state, and orbital hybridization that govern adsorption energetics. Moving beyond trial and error requires integrating high throughput DFT screening with machine learning to establish quantitative structure property relationships, and developing synthesis methods that can realize predicted atomic configurations with site specific precision.

Interfacial electron transport issues severely impair the efficiency and stability of electrocatalytic reactions. Methods such as interface engineering, bulk water redox chemistry, and pulsed electrocatalysis strategies can optimize interfacial electron transport and improve electrocatalytic performance. The recently discovered role of bulk water as an active redox

medium opens new paradigms for radical-mediated pathways that bypass traditional interfacial limitations. However, the solid–liquid interface is not static. Its electronic properties fluctuate with the electric double layer, local pH, and intermediate accumulation. Future research should combine *in situ* spectroscopies with time-resolved electrochemical measurements to track transient charge redistribution and intermediate speciation during reactions. Designing adaptive interfaces that self-regulate their electronic properties represents a frontier direction for stabilizing low impedance, poisoning resistant interfaces under industrially relevant conditions.

The lag in theoretical research constitutes a major bottleneck hindering the development of the electrocatalysis field. The advancement of theoretical approaches, including GCE-DFT and the new paradigm of asymmetric electrocatalyst design, provides novel theoretical frameworks and methodological guidance for electrocatalytic research. These methods enable simulations under constant potential and offer pathways to break linear scaling relations through deliberate symmetry breaking. However, realistic simulations of the electrochemical interface remain incomplete. Priorities for theoretical development include incorporating explicit solvation and dynamic surface reconstruction into constant potential frameworks, modeling the influence of the electric double layer structure on electron transfer kinetics and using machine learned force fields to simulate long timescale evolution of active sites under operating potentials. The ultimate aim is to predict catalyst performance before synthesis, accelerating the discovery of materials with optimized electronic properties.

In summary, the future of electrocatalysis lies in deepening our fundamental understanding of electronic phenomena and translating that knowledge into design principles. By concentrating on the four issues outlined above, the field can move toward the rational creation of catalysts with unprecedented efficiency and selectivity. This approach will ultimately provide a scientific foundation for the technological breakthroughs needed for sustainable energy conversion.

Author contributions

L. W. and J. L. supervised the research. J. L. conceived the review. H. S. contributed to investigation, data curation, collecting literature, and writing-original draft. Y. L. contributed to supervision and writing-review and editing. S. P. contributed to supervision and writing-review and editing. A. M. contributed to supervision and writing-review and editing. All authors discussed the results and commented on the manuscript.

Conflicts of interest

The authors declare no competing interests.

Data availability

No primary research results, software or codes have been included, and no new data were generated or analysed as a part of this review.

Code availability: all codes supporting the findings of this study are available from the corresponding author on request.

Acknowledgements

This work was supported by the National Natural Science Foundation of China (52272222), the Taishan Scholar Young Talent Program (tsqn201909114 and tsqn201909123), and the University Youth Innovation Team of Shandong Province (202201010318).

References

1 J. A. Blázquez, R. R. Maça, O. Leonet, E. Azaceta, A. Mukherjee, Z. Zhao-Karger, Z. Li, A. Kovalevsky, A. Fernández-Barquín, A. R. Mainar, P. Jankowski, L. Rademacher, S. Dey, S. E. Dutton, C. P. Grey, J. Drews, J. Häcker, T. Danner, A. Latz, D. Sotta, M. R. Palacin, J.-F. Martin, J. M. G. Lastra, M. Fichtner, S. Kundu, A. Kraytsberg, Y. Ein-Eli, M. Noked and D. Aurbach, A practical perspective on the potential of rechargeable Mg batteries, *Energy Environ. Sci.*, 2023, **16**, 1964–1981.

2 J. Li, Z. Li, Q. Sun, Y. Wang, Y. Li, Y. K. Peng, Y. Li, C. Zhang, B. Liu and Y. Zhao, Recent advances in the large-scale production of photo/electrocatalysts for energy conversion and beyond, *Adv. Energy Mater.*, 2024, **14**, 2402441.

3 S. Zhang, Z. Wu, Z. Liu and Z. Hu, An emerging energy technology: self-uninterrupted electricity power harvesting from the sun and cold space, *Adv. Energy Mater.*, 2023, **13**, 2300260.

4 X. Zhang, L. Hou, A. Ciesielski and P. Samorì, 2D materials beyond graphene for high-performance energy storage applications, *Adv. Energy Mater.*, 2016, **6**, 1600671.

5 S. W. Boettcher and Y. Surendranath, Heterogeneous electrocatalysis goes chemical, *Nat. Catal.*, 2021, **4**, 4–5.

6 A. Ghatak, G. S. Shanker, Y. Pearlmutter, A. Fryder, R. Shimoni and I. Hod, Dual molecular catalyst-based tandem that enables electrocatalytic CO_2-formaldehyde-methanol cascade conversion, *J. Am. Chem. Soc.*, 2025, **147**, 20329–20337.

7 A. J. Martín and J. Pérez-Ramírez, Heading to distributed electrocatalytic conversion of small abundant molecules into fuels, chemicals, and fertilizers, *Joule*, 2019, **3**, 2602–2621.

8 G. Centi and S. Perathoner, Electrocatalysis: prospects and role to enable an E-chemistry future, *Chem. Rec.*, 2025, **25**, e202400259.

9 E. P. Delmo, Y. Wang, Y. Song, S. Zhu, H. Zhang, H. Xu, T. Li, J. Jang, Y. Kwon, Y. Wang and M. Shao, In situ infrared spectroscopic evidence of enhanced electrochemical CO_2 reduction and C-C coupling on oxide-derived copper, *J. Am. Chem. Soc.*, 2024, **146**, 1935–1945.

10 R. Ding, J. Chen, Y. Chen, J. Liu, Y. Bando and X. Wang, Unlocking the potential: machine learning applications in electrocatalyst design for electrochemical hydrogen energy transformation, *Chem. Soc. Rev.*, 2024, **53**, 11390–11461.

11 F. Greenwell, B. Siritanaratkul, P. K. Sharma, E. H. Yu and A. J. Cowan, Pulsed electrolysis with a nickel molecular catalyst improves selectivity for carbon dioxide reduction, *J. Am. Chem. Soc.*, 2023, **145**, 15078–15083.
12 J. Lin, Z. Liu, H. Wu, Z. Wang, G. Wang, J. Bu, Y. Wang, P. Liu, J. Wang and J. Zhang, Efficient electroreduction of carbonyl compounds to alcohols over Fe/Fe_2O_3 interfaces, *Nat. Catal.*, 2025, **8**, 338–347.
13 Q. Sha, S. Wang, L. Yan, Y. Feng, Z. Zhang, S. Li, X. Guo, T. Li, H. Li, Z. Zhuang, D. Zhou, B. Liu and X. Sun, 10,000-h-stable intermittent alkaline seawater electrolysis, *Nature*, 2025, **639**, 360–367.
14 Y. Wang, H. Xu, Y. Liu, J. Jang, X. Qiu, E. P. Delmo, Q. Zhao, P. Gao and M. Shao, A sulfur-doped copper catalyst with efficient electrocatalytic formate generation during the electrochemical carbon dioxide reduction reaction, *Angew. Chem., Int. Ed.*, 2024, **63**, e202313858.
15 W. Xue, H. Jiang, J. Liu, X. Chen, C. Tang, B. Y. Xia and B. You, Bipolar ethylene electrosynthesis from CO_2 and biowaste acid with total faradaic efficiency over 118%, *Nat. Commun.*, 2025, **16**, 9054.
16 X. Wang, M. Yu and X. Feng, Electronic structure regulation of noble metal-free materials toward alkaline oxygen electrocatalysis, *eScience*, 2023, **3**, 100141.
17 L. Yang, X. Cao, X. Wang, Q. Wang and L. Jiao, Regulative electronic redistribution of $CoTe_2$/CoP heterointerfaces for accelerating water splitting, *Appl. Catal., B*, 2023, **329**, 122551.
18 W. Zhao, P. Du, Z. Gao, Y. Lv, S. Wang, G. Han, S. Li, S. Zhuang, M. Ma, Y. Lu, Z. Fang and Y. Hou, Magnetic free-standing electrodes achieving efficient oxygen evolution reaction via electronic structure regulation, *Adv. Energy Mater.*, 2026, e05577.
19 J. Huang, L. Sementa, Z. Liu, G. Barcaro, M. Feng, E. Liu, L. Jiao, M. Xu, D. Leshchev, S.-J. Lee, M. Li, C. Wan, E. Zhu, Y. Liu, B. Peng, X. Duan, W. A. Goddard, A. Fortunelli, Q. Jia and Y. Huang, Experimental Sabatier plot for predictive design of active and stable Pt-alloy oxygen reduction reaction catalysts, *Nat. Catal.*, 2022, **5**, 513–523.
20 C. Wei, Y. Sun, G. G. Scherer, A. C. Fisher, M. Sherburne, J. W. Ager and Z. J. Xu, Surface composition dependent ligand effect in tuning the activity of Nickel-Copper bimetallic electrocatalysts toward hydrogen evolution in alkaline, *J. Am. Chem. Soc.*, 2020, **142**, 7765–7775.
21 F.-Y. Chen, Z.-Y. Wu, Z. Adler and H. Wang, Stability challenges of electrocatalytic oxygen evolution reaction: from mechanistic understanding to reactor design, *Joule*, 2021, **5**, 1704–1731.
22 Z. Li, X. Zhang, H. Cheng, J. Liu, M. Shao, M. Wei, D. G. Evans, H. Zhang and X. Duan, Confined synthesis of 2D nanostructured materials toward electrocatalysis, *Adv. Energy Mater.*, 2019, **10**, 1900486.
23 D. Xu, K. Li, B. Jia, W. Sun, W. Zhang, X. Liu and T. Ma, Electrocatalytic CO_2 reduction towards industrial applications, *Carbon Energy*, 2022, **5**, e230.
24 W. Chang, A. Jain, F. Rezaie and K. Manthiram, Lithium-mediated nitrogen reduction to ammonia via the catalytic solid–electrolyte interphase, *Nat. Catal.*, 2024, **7**, 231–241.
25 X. Wang, Q. Yang, S. Singh, H. Borrmann, V. Hasse, C. Yi, Y. Li, M. Schmidt, X. Li, G. H. Fecher, D. Zhou, B. Yan and C. Felser, Topological semimetals with intrinsic chirality as spin-controlling electrocatalysts for the oxygen evolution reaction, *Nat. Energy*, 2024, **10**, 101–109.
26 J. Zhang, C. Zhang, M. Wang, Y. Mao, B. Wu, Q. Yang, B. Wang, Z. Mi, M. Zhang, N. Ling, W. R. Leow, Z. Wang and Y. Lum, Isotopic labelling of water reveals the hydrogen transfer route in electrochemical CO_2 reduction, *Nat. Chem.*, 2025, **17**, 334–343.
27 H. Li, J. Lai, Z. Li and L. Wang, Multi-sites electrocatalysis in high-entropy alloys, *Adv. Funct. Mater.*, 2021, **31**, 2106715.
28 H. Li, M. Sun, Y. Pan, J. Xiong, H. Du, Y. Yu, S. Feng, Z. Li, J. Lai, B. Huang and L. Wang, The self-complementary effect through strong orbital coupling in ultrathin high-entropy alloy nanowires boosting pH-universal multifunctional electrocatalysis, *Appl. Catal. B Environ. Energy*, 2022, **312**, 121431.
29 D. Zhang, Y. Shi, X. Chen, J. Lai, B. Huang and L. Wang, High-entropy alloy metallene for highly efficient overall water splitting in acidic media, *Chin. J. Catal.*, 2023, **45**, 174–183.
30 B. Deng, G. Yu, W. Zhao, Y. Long, C. Yang, P. Du, X. He, Z. Zhang, K. Huang, X. Li and H. Wu, A self-circulating pathway for the oxygen evolution reaction, *Energy Environ. Sci.*, 2023, **16**, 5210–5219.
31 X. Lang, Y. Jia, Q. Fang, Z. Peng, D. Zhong, J. Li and Q. Zhao, Engineering CuIn microenvironment for efficient acidic electrochemical CO_2 reduction to CO, *Appl. Catal. B Environ. Energy*, 2025, **371**, 125244.
32 W. Li, Y. Liu, A. Azam, Y. Liu, J. Yang, D. Wang, C. C. Sorrell, C. Zhao and S. Li, Unlocking efficiency: minimizing energy loss in electrocatalysts for water splitting, *Adv. Mater.*, 2024, **36**, 2404658.
33 W. Ma, J. Morales-Vidal, J. Tian, M.-T. Liu, S. Jin, W. Ren, J. Taubmann, C. Chatzichristodoulou, J. Luterbacher, H. M. Chen, N. López and X. Hu, Encapsulated Co-Ni alloy boosts high-temperature CO_2 electroreduction, *Nature*, 2025, **641**, 1156–1161.
34 L. Su, Q. Hua, Y. Yang, H. Mei, J. Li, G. Feng and Z. Huang, Regulating competing reaction pathways for efficient CO_2 electroreduction in acidic conditions, *J. Energy Chem.*, 2025, **105**, 326–351.
35 X. Lu, J. Wu, X. He, Z. Li, Y. Lu, W. Li, J. Li, M. Xu, Y. Qi, Q. Zhang, Y. Liu, M. Du, T. Kamiya, H. Hosono, F. Pan, J.-S. Chen and T.-N. Ye, Ordered single active sites for cascade hydrogenation and hydroformylation reactions, *Nat. Catal.*, 2025, **8**, 536–547.
36 D. Lv, R. Bai, Y. Deng, W. Zhao, Z. Xing, X. Liu, C. Ma, Q. Ma, Z. Mao, T. Zhang, K. Qi, W. Huang, Z. Q. Rong, X. Li, Y. Fang and J. Zhang, Dual spatial and electronic regulation in van der waals Cu_3Se_2 nanosheets for electrocatalytic acetylene semi-hydrogenation, *Angew. Chem., Int. Ed.*, 2025, e202516180.

37 G. Zhang, Q. Li, X. Wang, L. Jin and Q. Liao, Diverse behaviors of N_2 on Mo centers bearing POCOP-pincer ligands and the role of π-electron configuration in regulating the pathway of N_2 activation, *J. Am. Chem. Soc.*, 2025, **147**, 3747–3757.

38 K. Zhang, J. Wang, W. Zhang, D. Xiao, H. Yin, Z. Lu, M. Fan, W. Fan, Y. Zhang and P. Zhang, Adjusted preferential adsorption of intermediates via regulation of the electronic structure during the electrocatalytic CO_2 reduction process, *J. Phys. Chem. Lett.*, 2023, **15**, 34–42.

39 K.-M. Zhao, D.-X. Wu, W.-K. Wu, J.-B. Nie, F.-S. Geng, G. Li, H.-Y. Shi, S.-C. Huang, H. Huang, J. Zhang, Z.-Y. Zhou, Y.-C. Wang and S.-G. Sun, Identifying high-spin hydroxyl-coordinated $Fe^{3+}N_4$ as the active centre for acidic oxygen reduction using molecular model catalysts, *Nat. Catal.*, 2025, **8**, 422–435.

40 H. Zhu, X. Lv, Y. Wu, W. Wang, Y. Wu, S. Yan and Y. Chen, Carbonate-carbonate coupling on platinum surface promotes electrochemical water oxidation to hydrogen peroxide, *Nat. Commun.*, 2024, **15**, 8846.

41 Z. Cui, D. Wang, J. Ma, J. Guo, L. Li, Q. Nian, D. Ruan, B. Zhong, J. Fan, Z. Wang, J. Yang, X. Luo, Q. Dong, X. Ou, S. Jiao, R. Cao and X. Ren, Harnessing rapid Li^+/$H^{\delta+}$ exchange within the electric double layer for high performance Li-ion batteries, *Adv. Mater.*, 2025, **37**, e09735.

42 M. A. Gebbie, B. Liu, W. Guo, S. R. Anderson and S. G. Johnstone, Linking electric double layer formation to electrocatalytic activity, *ACS Catal.*, 2023, **13**, 16222–16239.

43 C. López, R. Rurali and C. Cazorla, How concerted are ionic hops in inorganic solid-state electrolytes?, *J. Am. Chem. Soc.*, 2024, **146**, 8269–8279.

44 Y. Wang, S. Zhou, Y. Zheng, Y. Wang, Y. Hou, K. Wu, C. Huang, S. Liu, Y. Shen, R. Chen and Y. Zhang, Measurements of local pH gradients for electrocatalysts in the oxygen evolution reaction by electrochemiluminescence, *J. Am. Chem. Soc.*, 2025, **147**, 19380–19390.

45 S. Zhou, K. S. Panse, M. H. Motevaselian, N. R. Aluru and Y. Zhang, Three-dimensional molecular mapping of ionic liquids at electrified interfaces, *ACS Nano*, 2020, **14**, 17515–17523.

46 X. Bai, X. Zhao, Y. Zhang, C. Ling, Y. Zhou, J. Wang and Y. Liu, Dynamic stability of copper single-atom catalysts under working conditions, *J. Am. Chem. Soc.*, 2022, **144**, 17140–17148.

47 T. Demeyere and C.-K. Skylaris, A comparison of modern solvation models for oxygen reduction at the Pt(111) interface, *J. Phys. Chem. C*, 2024, **128**, 19586–19600.

48 J. Huang, A. H. Clark, N. Hales, K. Crossley, J. Guehl, R. Skoupy, T. J. Schmidt and E. Fabbri, Oxidation of interfacial cobalt controls the pH dependence of the oxygen evolution reaction, *Nat. Chem.*, 2025, **17**, 856–864.

49 C. F. Yang, Y. Cui and D. M. Tartakovsky, Microkinetic models of electrochemistry: assumptions, limitations, and failures, *J. Phys. Chem. C*, 2025, **129**, 17080–17090.

50 D. Zhang, Y. Shi, H. Zhao, W. Qi, X. Chen, T. Zhan, S. Li, B. Yang, M. Sun, J. Lai, B. Huang and L. Wang, The facile oil-phase synthesis of a multi-site synergistic high-entropy alloy to promote the alkaline hydrogen evolution reaction, *J. Mater. Chem. A*, 2021, **9**, 889–893.

51 D. Zhang, H. Zhao, X. Wu, Y. Deng, Z. Wang, Y. Han, H. Li, Y. Shi, X. Chen, S. Li, J. Lai, B. Huang and L. Wang, Multisite electrocatalysts boost pH-universal nitrogen reduction by high-entropy alloys, *Adv. Funct. Mater.*, 2020, **31**, 2006939.

52 J.-N. Hu, L.-C. Tian, H. Wang, Y. Meng, J.-X. Liang, C. Zhu and J. Li, Theoretical screening of single-atom electrocatalysts of MXene-supported 3d-metals for efficient nitrogen reduction, *Chin. J. Catal.*, 2023, **52**, 252–262.

53 B. Y. Tang, R. P. Bisbey, K. M. Lodaya, W. L. Toh and Y. Surendranath, Reaction environment impacts charge transfer but not chemical reaction steps in hydrogen evolution catalysis, *Nat. Catal.*, 2023, **6**, 339–350.

54 J. Zang, W. Ye, Q. Liu, J. Meng and W. Yang, Plasmonic-promoted formation of surface adsorbed stochastic CO during electrochemical CO_2 and CO reduction on Cu at extreme low overpotentials, *J. Am. Chem. Soc.*, 2025, **147**, 10260–10267.

55 Y.-C. Liu, J.-R. Huang, H.-L. Zhu, X.-F. Qiu, C. Yu, X.-M. Chen and P.-Q. Liao, Electrosynthesis of pure urea from pretreated flue gas in a proton-limited environment established in a porous solid-state electrolyte electrolyser, *Nat. Nanotechnol.*, 2025, **20**, 907–913.

56 X. Ren, F. Liu, H. Wu, Q. Lu, J. Zhao, Y. Liu, J. Zhang, J. Mao, J. Wang, X. Han, Y. Deng and W. Hu, Reconstructed bismuth oxide through in situ carbonation by carbonate-containing electrolyte for highly active electrocatalytic CO_2 reduction to formate, *Angew. Chem., Int. Ed.*, 2024, **63**, e202316640.

57 Y. N. Xu, J. h. Li, J. C. Wu, W. Li, Y. Yang, H. Wu, H. Q. Fu, M. Zhu, X. L. Wang, S. Dai, C. Lian, P. F. Liu and H. G. Yang, Orbital matching mechanism-guided synthesis of Cu-based single atom alloys for acidic CO_2 electroreduction, *Adv. Mater.*, 2025, **37**, 2500343.

58 Y. Cheng, X. Zhou, Q.-M. Pan, L.-F. Zhang, Y.-F. Cao and T. Qian, Bimetallic active site nuclear-shell heterostructure enables efficient dual-functional electrocatalysis in alkaline media, *Rare Met.*, 2023, **42**, 3024–3033.

59 D. Feng, P. Wang, B. Ma, X. Zhao and Y. Chen, MoN@NiO core-shell heterostructure nanorods array for highly efficient electrocatalytic hydrogen evolution reaction, *Appl. Catal. B Environ. Energy*, 2025, **374**, 125373.

60 Y. Liu, Y. Huang, D. Wu, H. Jang, J. Wu, H. Li, W. Li, F. Zhu, M. G. Kim, D. Zhou, X. Xi, Z. Lei, Y. Zhang, Y. Deng, W. Yan, M. D. Gu, J. Jiang, S. Jiao and R. Cao, Ultrathin and conformal depletion layer of core/shell heterojunction enables efficient and stable acidic water oxidation, *J. Am. Chem. Soc.*, 2024, **146**, 26897–26908.

61 J. Feng, L. Wu, S. Liu, L. Xu, X. Song, L. Zhang, Q. Zhu, X. Kang, X. Sun and B. Han, Improving CO_2-to-C_{2+}

product electroreduction efficiency via atomic lanthanide dopant-induced tensile-strained CuO_x catalysts, *J. Am. Chem. Soc.*, 2023, **145**, 9857–9866.

62 Y. Wang, Y. Qin, R. Wen, L. Wang, M. Dou and F. Wang, High-performance low-iridium catalyst for water oxidation: breaking long-ranged order of IrO_2 by neodymium doping, *Small*, 2024, **20**, 2401964.

63 K. Surjith, D. Harsha, R. Vishnuraj and M. Rangarajan, 0D-3D-1D nanoarchitectured CQDs modified NiFe layered double hydroxides supported with MWCNTs: enhanced electrocatalytic performance for oxygen evolution reaction, *Int. J. Hydrogen Energy*, 2025, **97**, 798–812.

64 W. Li, Z. Wei, B. Wang, Y. Liu, H. Song, Z. Tang, B. Yang and S. Lu, Carbon quantum dots enhanced the activity for the hydrogen evolution reaction in ruthenium-based electrocatalysts, *Mater. Chem. Front.*, 2020, **4**, 277–284.

65 M. Singh, J. Park, H. Kim, G. Kim, D. Cha, D. R. Paudel, B. H. Kim and S. Lee, Heterointerface-driven electronic modulation in MoO_2@N/Mo–ReS_2 hybrid for efficient alkaline HER, OER, and overall water splitting, *Small*, 2025, **21**, 2505906.

66 Y. Wang, B. Tian, J. Zhuo, X. Ma, Y. Tian, W. Wang, Y. Liu and J. Hou, Dual regulation of interfacial proton transport and alloy electronic structure in Cu-In-(COOH)CNTs catalysts for selective CO_2 electroreduction, *J. Environ. Chem. Eng.*, 2025, **13**, 118231.

67 N. Luo, A. Cai, J. Pei, X. Zeng, X. Wang and N. Yao, Unveiling oxygen vacancy engineering in CoMo-based catalysts for enhanced oxygen evolution reaction activity, *Adv. Funct. Mater.*, 2025, **35**, 2425503.

68 M. Yu, A. Li, E. Kan and C. Zhan, Substantial impact of spin state evolution in OER/ORR catalyzed by Fe–N–C, *ACS Catal.*, 2024, **14**, 6816–6826.

69 K. Zhang, J. Wang, W. Zhang, H. Yin, J. Han, X. Yang, W. Fan, Y. Zhang and P. Zhang, Regulated surface electronic states of CuNi nanoparticles through metal-support interaction for enhanced electrocatalytic CO_2 reduction to ethanol, *Small*, 2023, **19**, 2300281.

70 Y. T. Wang, S. M. Wu, G. Q. Luo, S. T. Xiao, F. F. Pu, L. Y. Wang, G. G. Chang, G. Tian and X. Y. Yang, Dual Pd-acid sites confined in a hierarchical core-shell structure for hydrogenation of nitrobenzene, *Chem.–Asian J.*, 2023, **18**, e202300689.

71 Y. Cao, S. Chen, S. Bo, W. Fan, J. Li, C. Jia, Z. Zhou, Q. Liu, L. Zheng and F. Zhang, Single atom Bi decorated copper alloy enables C-C coupling for electrocatalytic reduction of CO_2 into C_{2+} products, *Angew. Chem., Int. Ed.*, 2023, **62**, e202303048.

72 X. Gao, Y. Jiang, J. Liu, G. Shi, C. Yang, Q. Xu, Y. Yun, Y. Shen, M. Chang, C. Zhu, T. Lu, Y. Wang, G. Du, S. Li, S. Dai and L. Zhang, Intermediate-regulated dynamic restructuring at Ag-Cu biphasic interface enables selective CO_2 electroreduction to C_{2+} fuels, *Nat. Commun.*, 2024, **15**, 10331.

73 Z. Li, C. Wang, Y. Liang, H. Jiang, S. Wu, Z. Li, W. Xu, S. Zhu and Z. Cui, Boosting hydrogen evolution performance of nanoporous Fe-Pd alloy electrocatalyst by metastable phase engineering, *Appl. Catal. B Environ. Energy*, 2024, **345**, 123677.

74 Y. Yu, J. Han, H. Li, H. Diao, Y. Shi, G. Jin, H. Li, G. A. Bagliuk, L. Wang and J. Lai, CuPt alloy enabling the tandem catalysis for reduction of HCOOH and NO_3^- to urea at high current density, *Adv. Mater.*, 2025, **37**, 2419738.

75 G. Yang, Y. Jiao, H. Yan, Y. Xie, A. Wu, X. Dong, D. Guo, C. Tian and H. Fu, Interfacial engineering of MoO_2-FeP heterojunction for highly efficient hydrogen evolution coupled with biomass electrooxidation, *Adv. Mater.*, 2020, **32**, 2000455.

76 J. Jiang, B. Gong, G. Xu, T. Zhao, H. Ding, Y. Feng, Y. Li and L. Zhang, Electron regulation of CeO_2 on CoP multi-shell hetero-junction micro-sphere towards highly efficient water oxidation, *J. Colloid Interface Sci.*, 2024, **668**, 110–119.

77 B. Zhang, J. Li, Q. Song, X. Xu, W. Hou and H. Liu, Transferable active centers of strongly coupled MoS_2@Sulfur and molybdenum Co-doped g-C_3N_4 heterostructure electrocatalysts for boosting hydrogen evolution reaction in both acidic and alkaline media, *Inorg. Chem.*, 2021, **60**, 2604–2613.

78 P. Zhou, S. X. Guo, L. Li, T. Ueda, Y. Nishiwaki, L. Huang, Z. Zhang and J. Zhang, Selective electrochemical hydrogenation of phenol with earth-abundant Ni-MoO_2 heterostructured catalysts: effect of oxygen vacancy on product selectivity, *Angew. Chem., Int. Ed.*, 2023, **62**, e202214881.

79 X. Liu, J. Ge, S. Li, H. Yang, H. Tian, H. Liu, Y. Li, X. Zheng, Y. Tian, X. Cui and Q. Xu, Activating dynamic Zn-ZnO interface with controllable oxygen vacancy in CO_2 electroreduction for boosting CO production, *Green Chem.*, 2025, **27**, 6133–6144.

80 L. Du, L. B. Chen, X. Liu, C. C. Yang and Q. Jiang, Heterogeneous interface and vacancy engineering contribute to metastable catalysts for overall water splitting, *Acta Mater.*, 2025, **289**, 120934.

81 W. Duan, P. Zhang, Y. Xiahou, Y. Song, C. Bi, J. Zhan, W. Du, L. Huang, H. Möhwald and H. Xia, Regulating surface facets of metallic aerogel electrocatalysts by size-dependent localized ostwald ripening, *ACS Appl. Mater. Interfaces*, 2018, **10**, 23081–23093.

82 B. Han, C. E. Carlton, A. Kongkanand, R. S. Kukreja, B. R. Theobald, L. Gan, R. O'Malley, P. Strasser, F. T. Wagner and Y. Shao-Horn, Record activity and stability of dealloyed bimetallic catalysts for proton exchange membrane fuel cells, *Energy Environ. Sci.*, 2015, **8**, 258–266.

83 Z. Huang, F. Li, Y. Liu, S. Chen, Z. Wei and Q. Tang, The role of nitrogen sources and hydrogen adsorption on the dynamic stability of Fe-N-C catalysts in oxygen reduction reaction, *Chem. Sci.*, 2024, **15**, 1132–1142.

84 A. Ooi, T. Kanda and E. Tada, Toward in situ dissolution monitoring of platinum nanoparticles by optimized online inductively coupled plasma mass spectrometry measurement, *ACS Appl. Nano Mater.*, 2025, **8**, 7256–7266.

85 M. Tang, H. Yan, X. Zhang, Z. Zheng and S. Chen, Materials strategies tackling interfacial issues in catalyst layers of

proton exchange membrane fuel cells, *Adv. Mater.*, 2023, **37**, 2306387.

86 X. Zhang, P. Yu, D. Shen, B. Cai, T. Han, Y. Xie and L. Wang, Atomically dispersed tungsten enhances CO tolerance in electrocatalytic hydrogen oxidation by regulating the 5d-orbital electrons of platinum, *Adv. Powder Mater.*, 2025, **4**, 100288.

87 Y.-P. Ku, K. Kumar, A. Hutzler, C. Götz, M. Vorochta, M. T. Sougrati, V. Lloret, K. Ehelebe, K. J. J. Mayrhofer, S. Thiele, I. Khalakhan, T. Böhm, F. Jaouen and S. Cherevko, Impact of carbon corrosion and denitrogenation on the deactivation of Fe-N-C catalysts in alkaline media, *ACS Catal.*, 2024, **14**, 8576–8591.

88 L. Strandberg, V. Shokhen, M. Skoglundh and B. Wickman, Carbon support corrosion in PEMFCs followed by identical location electron microscopy, *ACS Catal.*, 2024, **14**, 8494–8504.

89 T. Xu, H. Huang, T. Lu, Z.-J. Wang, S. Zhu, H. Jin, J. Li, X. Zhou, J.-J. Lv and S. Wang, Monitoring of anodic corrosion on carbon-based gas diffusion layer in a flow cell, *Carbon*, 2023, **205**, 207–213.

90 Y. Ma, T. Xiao, K. Zhu, W. Zhang, Z. Yin, A. Dong, Z. Sun, D. Zhao and W. Li, Industry-level electrocatalytic CO_2 to CO enabled by 2D mesoporous Ni single atom catalysts, *Angew. Chem., Int. Ed.*, 2024, **64**, e202416629.

91 S. Lu, X. Li, G. Zhang and S. Wang, Unlocking single-atom induced electronic metal-support interactions in electrocatalytic one-electron water oxidation for wastewater purification, *Nat. Commun.*, 2025, **16**, 4346.

92 D. Wang, F. Lin, H. Luo, J. Zhou, W. Zhang, L. Li, Y. Wei, Q. Zhang, L. Gu, Y. Wang, M. Luo, F. Lv and S. Guo, Ir-O-Mn embedded in porous nanosheets enhances charge transfer in low-iridium PEM electrolyzers, *Nat. Commun.*, 2025, **16**, 181.

93 D. Liu, X. Li, S. Chen, H. Yan, C. Wang, C. Wu, Y. A. Haleem, S. Duan, J. Lu, B. Ge, P. M. Ajayan, Y. Luo, J. Jiang and L. Song, Atomically dispersed platinum supported on curved carbon supports for efficient electrocatalytic hydrogen evolution, *Nat. Energy*, 2019, **4**, 512–518.

94 H. Qin, Y. Ye, G. Lin, J. Zhang, W. Jia, W. Xia and L. Jiao, Regulating the electrochemical microenvironment of $Ni(OH)_2$ by Cr doping for highly efficient methanol electrooxidation, *ACS Catal.*, 2024, **14**, 16234–16244.

95 J.-H. Sun, F. Guo, X.-Y. Li, J. Yang and J.-F. Ma, Constructing Ni/MoN heterostructure nanorod arrays anchored on Ni foam for efficient hydrogen evolution reaction under alkaline conditions, *Sustain. Energy Fuels*, 2021, **5**, 5565–5573.

96 F. Xie, Y. Du, M. Lu, S. Yan and Z. Zou, Thermal-stimulated spin disordering accelerates water electrolysis, *Energy Environ. Sci.*, 2025, **18**, 1972–1983.

97 L. Li and C. Cui, Bulk water redox chemistry enables radical-mediated C-C coupling in CO_2 electroreduction, *Nat. Chem.*, 2025, DOI: 10.1038/s41557-025-01948-z.

98 H. Sun and J.-Y. Liu, A pulsed tandem electrocatalysis strategy for CO_2 reduction, *J. Am. Chem. Soc.*, 2025, **147**, 14388–14400.

99 W. Qiu, S. Qin, Y. Li, N. Cao, W. Cui, Z. Zhang, Z. Zhuang, D. Wang and Y. Zhang, Overcoming electrostatic interaction via pulsed electroreduction for boosting the electrocatalytic urea synthesis, *Angew. Chem., Int. Ed.*, 2024, **63**, e202402684.

100 L. Liu and H. Xiao, Inverted region in electrochemical reduction of CO_2 induced by potential-dependent pauli repulsion, *J. Am. Chem. Soc.*, 2023, **145**, 14267–14275.

101 Y. Cao, Y. Liu, X. Zheng, J. Yang, H. Wang, J. Zhang, X. Han, Y. Deng, G. Rupprechter and W. Hu, Quantifying asymmetric coordination to Correlate with oxygen reduction activity in Fe-based single-atom catalysts, *Angew. Chem., Int. Ed.*, 2025, **64**, e202423556.

102 L. Zhang, Q. Xu, L. Xia, W. Jiang, K. Wang, P. Cao, Q. Chen, M. Huang, F. P. García de Arquer and Y. Zhou, Asymmetrically tailored catalysts towards electrochemical energy conversion with non-precious materials, *Chem. Soc. Rev.*, 2025, **54**, 5108–5145.

103 J. Zhang, Z. Song, X. Yao, Y. Guan, Z. Huo, N. Chen, L. Zhang and X. Sun, Precisely constructing asymmetric triple atoms for highly efficient electrocatalysis, *Chem*, 2025, **11**, 102498.

104 A. Samanta and C. R. Raj, Oxygen electrocatalysis with mesoporous Co-N-C catalysts: towards understanding the active site and development of rechargeable Zn-Air batteries, *ChemElectroChem*, 2020, **7**, 2877–2887.

105 J. Yin, H. Chen, J. Qiu, W. Li, P. He, J. Li, I. A. Karimi, X. Lan, T. Wang and X. Wang, SurFF: a foundation model for surface exposure and morphology across intermetallic crystals, *Nat. Comput. Sci.*, 2025, **5**, 782–792.

106 Z. Lian, F. Dattila and N. López, Stability and lifetime of diffusion-trapped oxygen in oxide-derived copper CO_2 reduction electrocatalysts, *Nat. Catal.*, 2024, **7**, 401–411.